U-Pb baddeleyite geochronology and geochemistry of the White Mfolozi Dyke Swarm: unravelling the complexities of 2.70-2.66 Ga dyke swarms on the eastern Kaapvaal Craton, South Africa

Johan Rådman

Dissertations in Geology at Lund University,
Master's thesis, no 407
(45 hp/ECTS credits)

Department of Geology
Lund University
2014

U-Pb baddeleyite geochronology and geochemistry of the White Mfolozi Dyke Swarm: unravelling the complexities of 2.70-2.66 Ga dyke swarms on the eastern Kaapvaal Craton, South Africa

Master's thesis

Johan Rådman

Department of Geology
Lund University
2014

Contents

Cover Picture: Overview of the more than 20 m wide dyke JR03, which follows the Mhalutze River Valley for approximately 800 m. (Photo: Johan Rådman)

U-Pb baddeleyite dating of the White Mfolozi Dyke Swarm

JOHAN RÅDMAN

Rådman, J., 2014: U-Pb baddeleyite geochronology and geochemistry of the White Mfolozi Dyke Swarm: unravelling the complexities of 2.70-2.66 Ga dyke swarms on the eastern Kaapvaal Craton, South Africa. *Dissertations in Geology at Lund University*, No. 407, 31 pp. 45 hp (45 ECTS credits)

Abstract: Numerous mafic dykes of different generations and trends intrude the eastern part of the Kaapvaal Craton. On eastern Kaapvaal, there are three previously investigated dyke swarms that appear to radiate out from the eastern lobe of the Bushveld Complex. The NE- and E trending branches comprise dykes dated at ca. 2660 Ma, 2685 Ma and 2700 Ma (Olsson et al. 2011). Further south, a NE-trending swarm, here named the White Mfolozi Dyke Swarm (WMDS), appears to cross cut the ca. 2700 Ma SE trending branch of the radiating swarm. New U-Pb baddeleyite ages for seven dykes of the WMDS are presented. The three most robust results yield a weighted mean age of 2661.8 ± 2.0 Ma (MSWD = 0.3), taken as a mean age of the WMDS. Taking the errors of the U-Pb results into account, the results do not rule out the possibility that emplacement of dykes was of very short duration (1 Myr, or even less). These results are identical in age to the NE- and E-trending dykes of the radiating swarm further north, indicating a possible more extensive event at ca. 2660 Ma. These results also cast some doubt on the interpretation of Olsson et al. (2011), i.e. that the radiating dykes were linked to a mantle plume that caused dyking over a 40 Myr time period (i.e. from 2700 to 2660 Ma). Rather, a maximum duration of 15 Myr appears to be a better estimate if assuming the 2660 Ma dykes instead belong to the WMDS, making this swarm up to 400 km in width. Another possibility is that there are two coeval but chemically different events. The ca. 2660 Ma dykes may be feeders to the lavas of the protobasinal fill sequence at the bottom of Transvaal Supergroup, dated to 2664 ± 1 Ma (U-Pb zircon; Barton et al. 1995).

The geochemistry of the ca. 2660 Ma WMDS are characterized by flat REE-patterns and overall depleted signatures, in contrast to its coeval more northerly dykes which are LREE enriched and show increasing crustal contamination. The 2660 Ma dyking event records either a spatially extensive common event during which magmas were more contaminated further north than in the south, or two spatially unrelated events.

Keywords: Kaapvaal Craton, White Mfolozi Dyke Swarm, geochronology, U-Pb, baddeleyite, Diabase, Dolerite

Supervisor: Ulf Söderlund **Co-supervisors:** Ashley Gumsley & Martin B. Klausen

Subject: Bedrock Geology

Johan Rådman, Department of Geology, Lund University, Sölvegatan 12, SE-223 62 Lund, Sweden.

U-Pb geokronologi för White Mfolozi Dyke Swarm

JOHAN RÅDMAN

Rådman, J., 2014: U-Pb dateringar och geokemiska undersökningar av White Mfolozi Dyke Swarm: en ny syn på de 2.70-2.66 miljarder år gamla mafiska gångsvärmarna i östra delen av Kaapvaal kratonen i Sydafrika. *Examensarbeten i geologi vid Lunds universitet*, Nr. 407, 31 sid. 45 hp .

Sammanfattning: Den östra delen av Kaapvaalkratonen i södra Afrika är rikt på flera generationer av mafiska gångar med olika riktningar. Där finns tre gångsvärmar som tidigare undersökts och som tillsammans bildar ett radierande mönster med ett gemensamt fokus i Bushveld-komplexets östra del. De nordostliga och ostliga grenarna av denna svärm består av diabasgångar som blivit daterade till ca 2660, 2685 och 2700 miljoner år (Olsson et al. 2011). Längre söder ut finns en annan nordöstlig gångsvärm, som i detta arbete döpts till White Mfolozi Dyke Swarm (WMDS). Denna svärm ser ut att skära den sydostliga grenen av den radierande gångsvärmen. Nya U-Pb dateringar på mineralet baddeleyit från sju olika diabasgångar i WMDS presenteras i detta arbete. Ett viktat medelvärde av de tre mest robusta dateringarna ger åldern 2661,8 ± 2.0 miljoner år (MSWD = 0,3). Denna ålder kan betraktas som en medelålder för WMDS. Med hänsyn till analytiska felen, går det inte att utesluta att denna gångsvärm intruderade jordskorpan väldigt snabbt, kanske på så kort tid som en miljon år eller mindre. Åldern för WMDS är identisk med de yngsta gångarna i de nordöstliga och östliga diabasgångarna längre norrut, vilket indikerar att händelsen som skapade dessa diabasgångar för ungefär 2660 miljoner år sedan hade större utbredning än vad man tidigare trott. Mina resultat ifrågasätter den tidigare tolkningen som Olsson et al. (2011) gjorde, d.v.s. att den radierande gångsvärmen var kopplad till en mantelplym som bildade diabasgångar under en utdragen period av 40 miljoner år (från 2700 till 2660 miljoner år). De nya resultaten indikerar att bildningen av diabasgångarna upphörde för ungefär 2685 miljoner år sedan, och att den maximala längden av den perioden snarare var ca 15 miljoner år. Denna tolkning förutsätter att alla diabasgångar med en ålder runt 2660 miljoner år bildades av samma tektoniska händelse och i så fall bildar en upp till 400 km bred svärm. De 2660 miljoner år gamla gångarna kan ha varit matargångar till de omfattande vulkanutbrotten som bildade basaltflöden (”protobasinal fills”) vilka utgör basen av lagerföljden i Transvaal Supergroup. Dessa är daterade till 2664 ± 1 miljoner år med U-Pb metoden på zirkon (Barton et al. 1995)

De ungefär 2660 miljoner år gamla WMDS är geokemiskt karaktäriserade av flacka REE-mönster och har generellt utarmade signaturer i jämförelse med de jämnåriga diabasgångarna längre norrut. Gångarna i norr är mera LREE-berikade och har generellt en kemi som tyder på omfattande kontaminering från jordskorpan. Händelsen som skapade diabasgångarna för 2660 miljoner år sedan visar på en storskalig magmatisk händelse där kontamineringen från jordskorpan påverkade gångarnas kemi längre norr än i söder. Alternativt representerar dessa diabasgång två helt orelaterade, men samtida, händelser.

Nyckelord: Kaapvaal, White Mfolozi Dyke Swarm, geokronologi, U-Pb, baddeleyit

Handledare: Ulf Söderlund **Biträdande handledare:** Ashley Gumsley & Martin B. Klausen

Ämnesinriktning: Berggrundsgeologi

Johan Rådman, Geologiska institutionen, Lunds Universitet, Sölvegatan 12, 223 62 Lund, Sverige.

1 Introduction

Throughout most of Earth's geological history, continents have constantly been moving across Earth's surface driven by plate tectonic processes. In cycles of approximately 500 Ma, supercontinents have been assembled, broken up and drifted apart (Nance et al. 2014). The most well-known and recent is Pangaea (300-180 Ma) (e.g. Bradley 2011). Earlier supercontinents include Rodinia (1100-600 Ma) (e.g. Li et al. 2008) and Columbia (also named Nuna, 1800-1500 Ma) (e.g. Zhang et al. 2012). There are reasons to think that originally all, or most of, Archaean crust was part of a single landmass (Kenorland) or a limited number of larger cratons (Bleeker, 2003). Vaalbara is one of the proposed cratons, proposed to encompass the Kaapvaal and Pilbara cratons. According to Bleeker (2003), the break-up of Vaalbara appears to predate the assembly of Kenorland.

Supercontinent reconstructions involve, among other methods, precise dating of mafic dyke swarms and sills. Swarms are emplaced parallel to the rifting during break-up of continents, or in a radiating pattern outward from magmatic centres (Ernst et al. 2008). Dyke swarms, especially those radiating, are often linked to the arrival of mantle plums forming Large Igneous Provinces (LIPs). The term LIP has been defined by Coffin and Eldholm (1994) as "massive crustal emplacements of predominantly mafic (Mg and Fe rich) extrusive and intrusive rock which originate via processes other than "normal" seafloor spreading". The dykes (and sills) represent the "plumbing" system for mantle-derived magmas as they ascend through the crust and erupt at Earth's surface. By studying remnants of LIPs, such as dykes and sills, continents can be traced back to former nearest neighbours through comparing the LIP barcode diagrams between two or more continents (Bleeker & Ernst 2006). In such diagram each dated dyke swarm is illustrated by a horizontal line, i.e. a bar. Multiple age matches shared indicate the cratons were adjacent ("next neighbours") and likely had a common geological history over the time interval matches occur.

Numerous mafic dykes with different trends and ages intrude the Archaean basement of the eastern and south-eastern Kaapvaal Craton. Recent studies using U-Pb geochronology of mafic dykes and sills in Kaapvaal have contributed to better constrain links to the Zimbabwe Craton (e.g. Söderlund et al. 2010) and Valbaara (Gumsley et al. in progress). This thesis reports new U-Pb baddeleyite ages and geochemistry for seven NE-trending dykes of the here called ''White Mfolozi Dyke Swarm'', which is a significant dyke swarm in the south-eastern portion of the Kaapvaal craton. The scope is to refine and expand the barcode record for the Kaapvaal Craton and to investigate geochronological and geochemical relationship between different (but almost) coeval dyke swarms along the eastern and south-eastern portion of the craton.

2 Geological setting

2.1 Regional geology

2.1.1 The basement

The Kaapvaal Craton in southern Africa is one of approximately 35 pieces of crust that was formed in the Archaean (Bleeker 2003). Together with the Pilbara Craton in north-western Australia, the Kaapvaal Craton is one of few cratons that has preserved relatively pristine rocks of Mesoarchaean age (e.g., De Wit et al. 1992). Since its formation and stabilisation at ca. 3.1 – 3.7 Ga (Brandl et al. 2006) the Kaapvaal Craton has experienced a complex evolution of tectono-magmatic events and basin formation from the Mesoarchaean to the Phanerozoic eons. The complex intrusive history begins in the Eoarchaean (> ca. 3.60 Ga), and extends to the end of the Mesozoic era (ca. 0.065 Ga) (Anhaeusser 2006, Uken & Watkeys 1997). Igneous intrusions are widespread throughout the Archaean basement rocks. Supracrustal sedimentary and volcanic rocks cover large parts of the craton, especially in its western and southern portions (Fig. 1).

In the eastern part of the Kaapvaal Craton, the biggest exposure of Archaean basement granite-greenstone terrain is found (Fig. 1). Here, the nucleus of the Kaapvaal Craton is exposed. It consists of the Ancient Gneiss Complex (AGC) in Swaziland, and the Barberton Greenstone Belt in South Africa (De Wit et al. 1992, Eglington & Armstrong 2004). Several series of granitoid sub-domains later amalgamated onto this nucleus to form the Witwatersrand Terrain of the Kaapvaal Craton (De Wit et al. 1992). Further south, in northern part of KwaZulu-Natal in South Africa, Archaean basement is exposed in isolated inliers. This area is referred to as the south-easternmost window of Archaean basement according to Klausen et al. (2010) and Lubnina et al. (2010) (Fig. 2). The Archaean basement is mostly covered by the sedimentary rocks of Karoo Supergroup, and the Mesoproterozoic rocks of the Namaqua-Natal Orogen to the south of them.

2.1.2 Sedimentary and volcanic supracrustal cover

On the Eo- to Mesoarchaean basement rocks of the Kaapvaal Craton, a number of sedimentary and volcanic supracrustal successions have been deposited. The oldest cover succession is the Dominion Group, which is interpreted to manifest a rifting event on the centre of the Kaapvaal Craton. It consists of 3074 ± 6 Ma felsic volcanics and overlying rift-filling clastic sedimentary rocks (Armstrong et al. 1991). The Dominion Group is unconformably overlain by the Witwatersrand and Ventersdorp Supergroups (Marsh 2006).

The Witwatersrand Supergroup is dominated by clastic sedimentary rocks which are generally upward coarsening and are thought to have been deposited in a fore-

land basin. It is host to the world's largest historical deposit of placer gold (McCarthy 2006). The age of these sedimentary rocks is uncertain, therefore the age of Witwatersrand sedimentation is bracketed between ca. 2970 and ca. 2714 (Armstrong et al. 1991 & McCarthy 2006).

East of the Witwatersrand Basin, the Pongola Supergroup overlies the basement on the south-eastern Kaapvaal Craton. This basin is composed of bi-modal volcanics of the Nsuze Group (Gold 2006) at its base. These are overlain by the Mozaan Group upward-coarsening clastic sedimentary sequence, which can be correlated with the West Rand and Central Rand Groups of the Witwatersrand Supergroup (Beukes & Cairncross 1991, Gold 2006). It is also possible that the Nsuze Group may be coeval with the Dominion Group (Cole 1994). A recent paper by Mukasa et al. (2013) established a maximum age of the Pongola Supergroup at 2980 ± 10 Ma (U-Pb on zircon from a lower Nsuze lava unit), and a minimum age of 2954 ± 9 Ma (U-Pb zircon on an upper Mozaan lava unit, the Tobolsk lava).

The Ventersdorp Supergroup is an over 5 km thick volcanic and sedimentary sequence deposited rapidly from 2714 to 2709 Ma (U-Pb from zircon in the lavas) (Armstrong et al. 1991). These ages have been questioned by de Kock et al. (2012) and Wingate (1998), who disagrees to the rapid deposition and argue that the U-Pb zircon age of ca. 2780 Ma on the Derdepoort basalt reflects the start of volcanism in the Ventersdorp Supergroup. The whole Ventersdorp sequence is deposited in a NE-trending rift structure (Stanistreet & McCarthy 1991), and the origin of its associated flood basalts is debated. Stanistreet and McCarthy (1991) related the flood basalts to the collision between Zimbabwe and Kaapvaal cratons, although Eriksson et al. (2002) argued it was emplaced as the result of a mantle plume event.

Unconformably overlying the Ventersdorp Supergroup is a series of protobasinal fills, a discrete sedimentary and volcanic sequence that is interpreted by Eriksson et al. (2001) to have been deposited in an E-W trending rift environment. The lava units have been dated to 2657-2659 Ma (unpublished report, SACS, 1993) and 2664 ± 0.7 Ma using U-Pb zircon (Barton et al. 1995). On top of these protobasinal fills lies the entire Transvaal Supergroup, a mainly sedimentary unit that was deposited over an almost 500 Myr time interval from ca. 2600-2100 Ma (Beukes and Gutzmer, 2006). Today it is preserved in three sub-basins across Kaapvaal Craton: the Transvaal and Kanye sub-basins in the north-east and north-west, and the third basin, the Griqualand West sub-basin, in the south-western craton, and is also where the youngest age obtained for a Transvaal unit stem from. Cornell et al. (1996) reported a 2222±13 Ma (Pb-Pb whole rock) age from the Ongeluk-Hekpoort Formation. However, much more sedimentary rock conformably overlies this volcanic unit, thus the Transvaal sedimentation continued for some time after ca. 2222 Ma.

The largest layered intrusion in the world, the economically important Bushveld Complex, intruded into the Transvaal Supergroup (Cawthorn et al. 2006). Several ages obtained by different analytical methods are reported in the literature for the Bushveld Complex. Olsson et al. (2010) reported the first U-Pb baddeleyite age for the Rustenburg Layered Suite, 2057.7±1.7 Ma.

Rock units younger than the Bushveld Complex are grouped together on the map (Fig. 1). These include among others the sedimentary Waterberg Group and rocks of the volcanic and sedimentary Soutpansberg Group. Both have a composite thickness of 7 km (Hanson et al. 2004). Younger, major magmatic events are the ca. 1.1 Ga Umkondo LIP (Hanson et al. 2006) and the ca. >0.18 Ga Karoo LIP (Duncan & Marsh 2006). The Karoo rocks cover large parts of the Kaapvaal Craton and its supracrustal successions, as well as large areas outside the Kaapvaal Craton in southern Africa. It is thought to be associated to a mantle plume, and consists of both extrusive and intrusive rocks (Duncan & Marsh 2006).

2.1.3 Mafic dykes swarms in the eastern and south-eastern Kaapvaal Craton

Regardless of their age, Archaean and Proterozoic diabase dyke swarms piercing the Kaapvaal Craton generally trend in NW-SE, E-W or NE-SW directions (Uken & Watkeys 1997). These authors also state that it is apparent that these main trends were initiated at different times, even if the trend of a certain dyke swarm does not necessarily reveal its age. Earlier regional fabrics and structures may have been reactivated during younger extensional events, hence having a control on the trends of dykes (Jourdan et al. 2004). Bleeker & Ernst (2006) proposed that dyke swarms on the Kaapvaal Craton presumably record continental-scale rifting events. Uken and Watkeys (1997) have for example suggested that the NE-trending structures were initiated by Ventersdorp rifting. This prominent NE trend is also observed for dyke swarms on both the eastern and south-easternmost basement windows of the Kaapvaal Craton.

In the eastern window, there are three distinct swarms that radiate out from the eastern lobe of the Bushveld Complex. Olsson et al. (2010) reports precise U-Pb ID-TIMS baddeleyite dates for dykes comprising all swarms. The northernmost swarm is called the Black Hills Dyke Swarm. It is composed of a number of NE- to NNE-trending dykes, of which most dykes have yielded dates in the at 1875-1835 Ma time span (Olsson 2012). The two other swarms, are the E-trending Rykoppies Dyke Swarm (2685.5±5.5 Ma) and the SE-trending Barberton-Badplaas Dyke Swarm (ca. 2966 Ma and 2698 Ma) (Olsson et al. 2010 & 2011).

However, there is also an older generation of NE-trending diabase dykes of the Black Hills swarm that is intermixed with the 1875-1835 Ma dykes. Olsson et al. (2011) obtained ages of 2659 ± 13 Ma, 2692.4 ± 1.4 Ma and 2701 ± 11 Ma on three of these

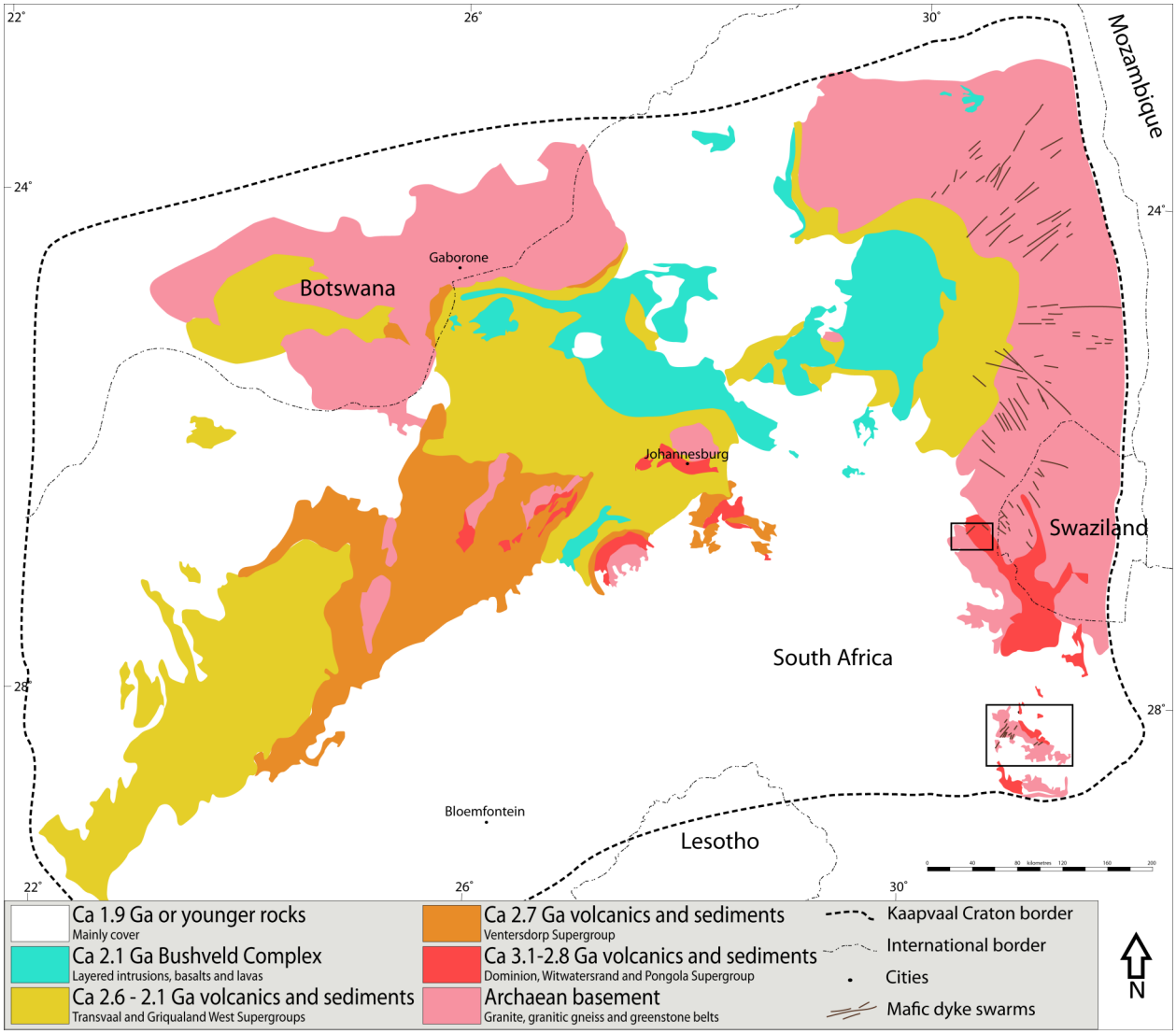

Fig. 1. A simplified geological map of the Kaapvaal Craton. The framed rectangles depict the study area. Modified from Frick (1997).

dykes (BCD5-22, 23 and 27). They are of approximately the same age as the Ventersdorp magmatic event. These Ventersdorp ages are repeated also within the E-W trending Rykoppies dyke swarm (Olsson et al. 2010).

Dolerite dykes and sills of Karoo age are also frequently found intruding the Kaapvaal Craton and its cover rocks. Generally, they are unaltered basaltic dolerites, compared to the Archaean and Proterozoic dykes which generally are more altered, basic to intermediate in composition (Uken & Watkeys 1997).

The south-easternmost window of Archaean basement is located in northern KwaZulu-Natal in South Africa at approximately 28° south in latitude. It is completely surrounded by the sedimentary rocks of the Karoo Supergroup. The Archaean basement here displays numerous mafic dyke intrusions of various trends, and sills probably of both Jurassic and Precambrian age (Klausen et al. 2010). Both Klausen et al. (2010) and Lubnina et al. (2010) stated that NE-trending and E- to ENE-trending dyke swarms dominate the area. The NE-trending dykes were also noted to cut the Pongola Supergroup in the area, but are absent in the Karoo cover. In the south-easternmost window, there is only one dyke which has been dated prior to this study. It is part of a SE-trending diabase dyke swarm consisting of ca. 2.87 Ga dykes dated by (Gumsley et al. 2013). The authors link this swarm to the coeval Hlagothi Complex, which is a series of layered sills abundant this region of the craton.

2.1.4 The White Mfolozi Dyke Swarm

The NE-trending diabase dyke swarm in the south-easternmost basement window is the focus of this study. The swarm was sampled in and around the White Mfolozi River, from which its name is derived, the 'White Mfolozi Dyke Swarm'. The swarm trends from 20° to 50° (N)NE and the feldspar phenocrysts are characteristic of this swarm, as was noted in Klausen et al. (2010). The phenocrysts vary in size from a few millimetres up to 10 cm in diameter. In

general, the NE-trending dykes are medium- to coarse-grained, and some of them show a chilled margin to their host rock. The width of the dykes vary, but all the samples used for this study are from dykes ca. 10-30 m across. The locations of the sampled dykes are shown in Fig. 2.

3 Field geology and petrography

During a field trip in October 2013, 19 samples were taken in the KwaZulu-Natal and Mpumalanga provinces of South Africa. Suitable diabase dykes were identified from using Google Earth over the Archaean inliers of the Kaapvaal Craton. Six sampled diabase dykes yielded a sufficient amount of baddeleyite for geochronology. One additional sample (BCD5-04) was collected on an earlier field trip, and the results of two fractions were reported by Olsson (2012). In this study, BDC5-04 was re-processed for baddeleyite, and two more fractions were analysed. All four analyses are included for calculation of the age of this sample. Coordinates for the sample sites are provided below . Samples were collected from dykes both in outcrop from exposed river pavements, on ridges and from weathered in situ boulders. Generally, when both contacts of the dyke with the country rock were exposed, the samples were taken from the central, more coarser, part of the dyke. If no visible contact could be seen, the samples were collected where the rock was the most coarse-grained, since the probability of finding baddeleyite is greatest in coarse rock.

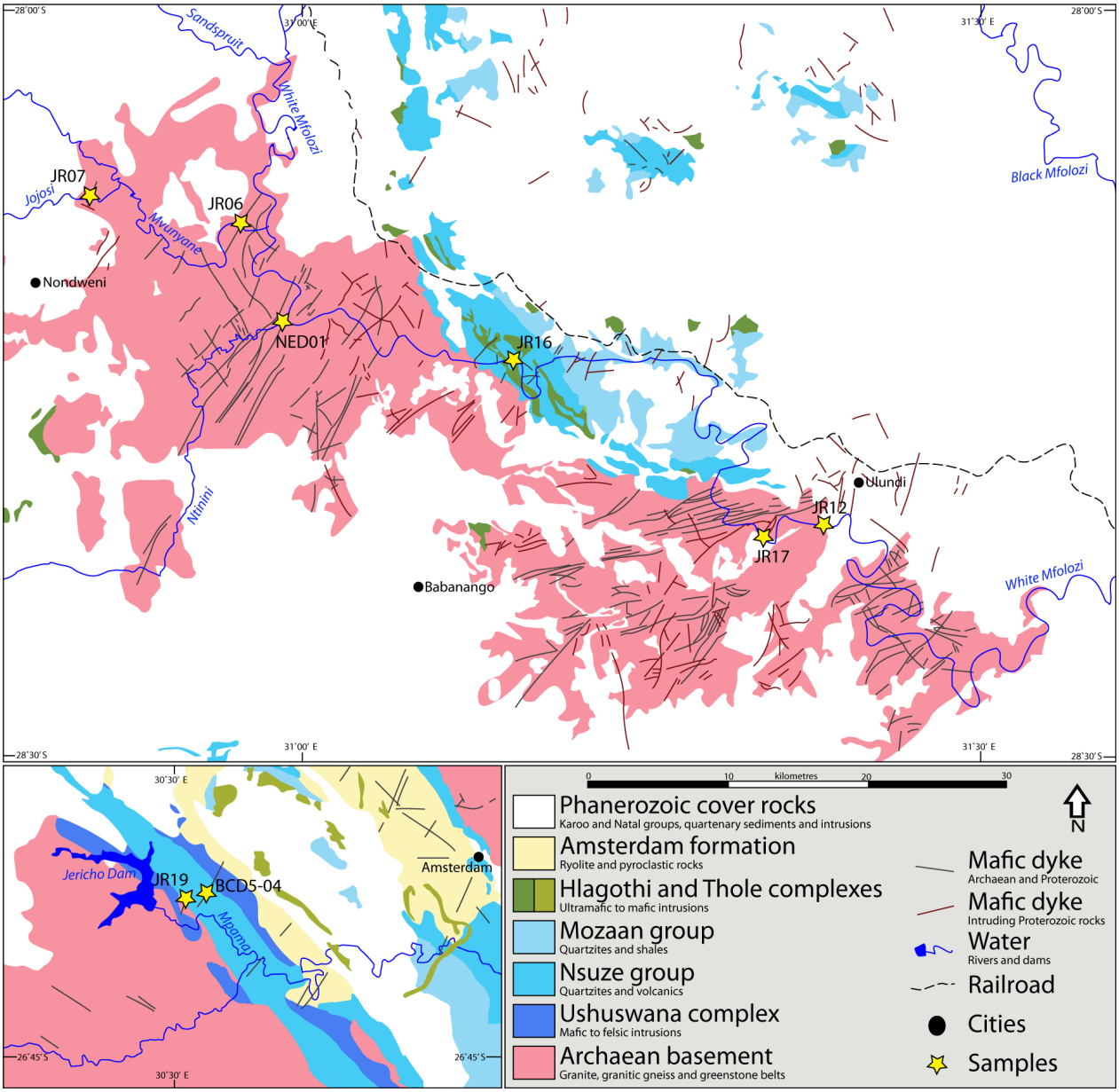

Fig. 2. Geological maps of the two study areas, which are highlighted in Fig. 1. The larger map shows the field area in northern KwaZulu-Natal, whereas the inset map shows the area in which samples JR19 and BCD5-04 were taken. They were sampled approximately 190 km north of the White Mfolozi River. JR03 are located south of the large map. Maps are modified after Linström (1987).

Polished thin sections were prepared from all the JR samples, and studied under optical microscope. No baddeleyites were found in JR03 and JR12, hence neither of these samples were dated. They are still assumed to belong to the White Mfolozi dyke swarm since they have similar trends, are rich in phenocrysts and and have similar mineralogies as the other dykes.

All samples have a common feature in that no olivine has been observed. All of them contain chlorite, indicative of lower greenschist facies metamorphism. Amphiboles are assumed to be secondary actinolite-tremolite through uralitization, but some hornblende may be primary.

South African tradition calls for older and slightly metamorphosed mafic dykes to be called diabase, while young and fresh dykes (i.e. from the Karoo event) are called dolerites.

3.1 JR03 (S 28.599170° 31.170300°E)

This dyke is over 20 m wide and follows the Mhalutze River for approximately 800 m (see cover page). The dyke has a more northerly trend of 016°, which is slightly different relative to other dykes of the swarm. Phenocrysts are mostly subhedral, numerous and evenly scattered, reaching up to 5 cm in size. The grain size varies across the dyke, but the central parts are mostly medium- to coarse-grained. The diabase dyke is cross-cut by a younger ESE-trending and more fine-grained mafic dyke (Fig. 3).

Fig. 3. JR03 is cross-cut by an ESE-trending dyke. Note the lack of feldspar phenocrysts in the ESE dyke below the dashed line. The lens cap is 7 cm in diameter.

Plagioclase laths are inter-connected almost throughout the entire thin section, resulting in a subophitic texture. Some plagioclase is strongly sericitized in the central parts of the crystals (Fig. 8a), which could possibly be explained by the cores being more Ca-rich than the rims. All clinopyroxene crystals show a slight green pleocroism in plane-polarized light, which indicate initial stages of uralitisation (Fig. 8b). Amphibole, some of which might be primary, exists together with clinopyroxene and chlorite in the groundmass. The groundmass also contains some opaque minerals and subordinate quartz.

3.2 JR06 (S 28.14558° E30.95492°)

This dyke is approximately 30 m wide and contains numerous white to pale pink feldspar phenocrysts. It outcrops in the Mvunyane River, approximately 2 km upstream from where it merges with the White Mfolozi River. The dyke has a trend of 048°. Most of the dyke is medium-grained, but the grain size decreases towards the contacts where a chilled margin is displayed along both contacts. The feldspar phenocrysts also decrease in size towards the contact. There are no phenocrysts at the north-western contact, while they appear all the way along the contact to the south-eastern side. The size of the phenocrysts varies from 0.5 cm to more than 10 cm, and they are euhedral to subhedral. Also rounded phenocrysts occur (Fig. 4). Some of the larger megacrysts show a rim of a pale white colour. There is no preferred orientation among them.

Fig. 4. Subhedral to euhedral feldspar phenocrysts occuring in a mixture of sizes in this 30 m wide dyke.

JR06 is a coarse-grained diabase where the plagioclase grains are prismatic but commonly strongly sericitized (Fig. 8c). Clinopyroxene is almost totally altered, but there are some remnants within secondary amphibole. This sample has a higher abundance of amphibole and chlorite than clinopyroxene. A few small quartz grains are present too. Clinopyroxene has broken down either to amphibole or a mixture of secondary brown-coloured minerals (Fig. 8d). Among them, some are chlorite, which appear more greenish in colour.

3.3 JR07 (S 28.12385° E30.84167)

This dyke was sampled along a ridge, shows no contacts to the host rock and consists of boulder scree (Fig. 5). Although not exposed in situ, the dyke follows a linear trend assumed to be the original dyke orientation from which the sample was obtained. The boulder scree reveals that the minimum width of the dyke is approximately 15 m. Its trend could be estimated to approximately 023° by visibly following the dyke downhill and across the Jojosi River to the south-west. Satellite imagery on Google Earth confirms this direction. The sample is medium- to coarse-grained and fresh. It contains anhedral feldspar phenocrysts of various sizes up to a few millimetres.

Fig. 5. JR07 was sampled on a ridge dyke crossing the Jojosi River, which can be seen in the background of this photo.

JR07 is a medium-grained diabase and has large phenocrysts of clinopyroxene. Most of them are altered or chemically zoned at the rims, which can be seen as changing interference colours when viewed in crossed polars (Fig. 8e). Some clinopyroxene only has the core intact. The altered rims are rich in fine-grained dark minerals showing low first-order interference colours, possibly chlorite. In this ophitic texture, there are traces of plagioclase laths (Fig. 8f), but not as much as is the other samples. The amphibole content is low too. The matrix consists mostly of plagioclase, subordinate quartz, amphibole and opaque minerals.

3.4 JR12 (S 28.339030° E 31.368800°)

This dyke trends 050° and is at least 10 m wide. It crops out as large boulders in the White Mfolozi River but its contact to the host rock is under the waterline or covered with sand in the river bed. Numerous feldspar phenocrysts of variable size (0.5 – 4 cm) are evenly spread over the outcrop (Fig. 6). Small mm-sized grains of pyrite are also frequent in this dyke. No baddeleyites were recovered from this sample for age dating.

JR12 displays variably altered clinopyroxene, and some compositional zoning, similar to that seen in JR07. Amphibole and chlorite are abundant as secondary minerals (Fig. 8g). Some grains of clinopyroxene appear with amphibole rims. There is also some amphibole that is primary. Plagioclase is mostly sericitized and occurs as large phenocrysts (Fig. 8h) in the groundmass of medium-grained plagioclase grains, pyroxene, amphibole, chlorite and accessory quartz and opaque minerals. Chlorite is more abundant than amphibole, and sometimes intermixed with secondary mica and/or oxides.

Fig. 6. The feldspar phenocrysts are of variable size in this dyke. They show no preferred orientation.

3.5 JR16 (S 28.23483° E 31.14790°)

In the White Mfolozi valley, this dyke crops out approximately 2.3 km west of Matatane River Lodge. It is ca. 25 m wide and strikes 050°. The dyke is medium- to coarse-grained and heavily populated with feldspar phenocrysts (Fig. 7). In the centre of the dyke the phenocrysts are 0.5-8 cm long, whereas towards the dyke contact, they are less than 1 cm. Even though the water level in the river was very low during sampling, the contacts to the host rock were mostly under water or covered by sand.

Fig. 7. Big phenocrysts intermixed with small ones in the centre of the dyke JR16.

In thin section, this sample appears as a coarse- to medium-grained diabase with strongly sericitized plagioclase crystals. It is almost entirely surrounded by primary mafic minerals or alteration products, with an ophitic texture. Clinopyroxene grains mainly show alteration throughout the grains, though some of them only at the rims however. Some twining is still visible (Fig. 8i). Amphibole is present, which may be of both primary (distinct cleavage visible) and secondary (no cleavage) in origin (Fig. 8j). This sample contains more quartz, but with less opaque minerals than the other samples in the groundmass. There are also plagioclase and pyroxene in the groundmass.

3.6 JR17 (S 28,35162° E 31,34177°)

This dyke crops out in the White Mfolozi river valley. It is a medium-grained dyke that is trending 023°. The contacts to its host rock are not visible, but the dyke is estimated to have a width of approximately 10 m.

Studying JR17 in thin section, it has intact cores of clinopyroxene (Fig. 8k), though most of the grains are altered, similar to JR16. Before metamorphism, clinopyroxene was probably the most dominant mineral occurring as large phenocrysts in a matrix dominated by plagioclase with accessory phases. Chlorite is abundant. Plagioclase is not as altered as in

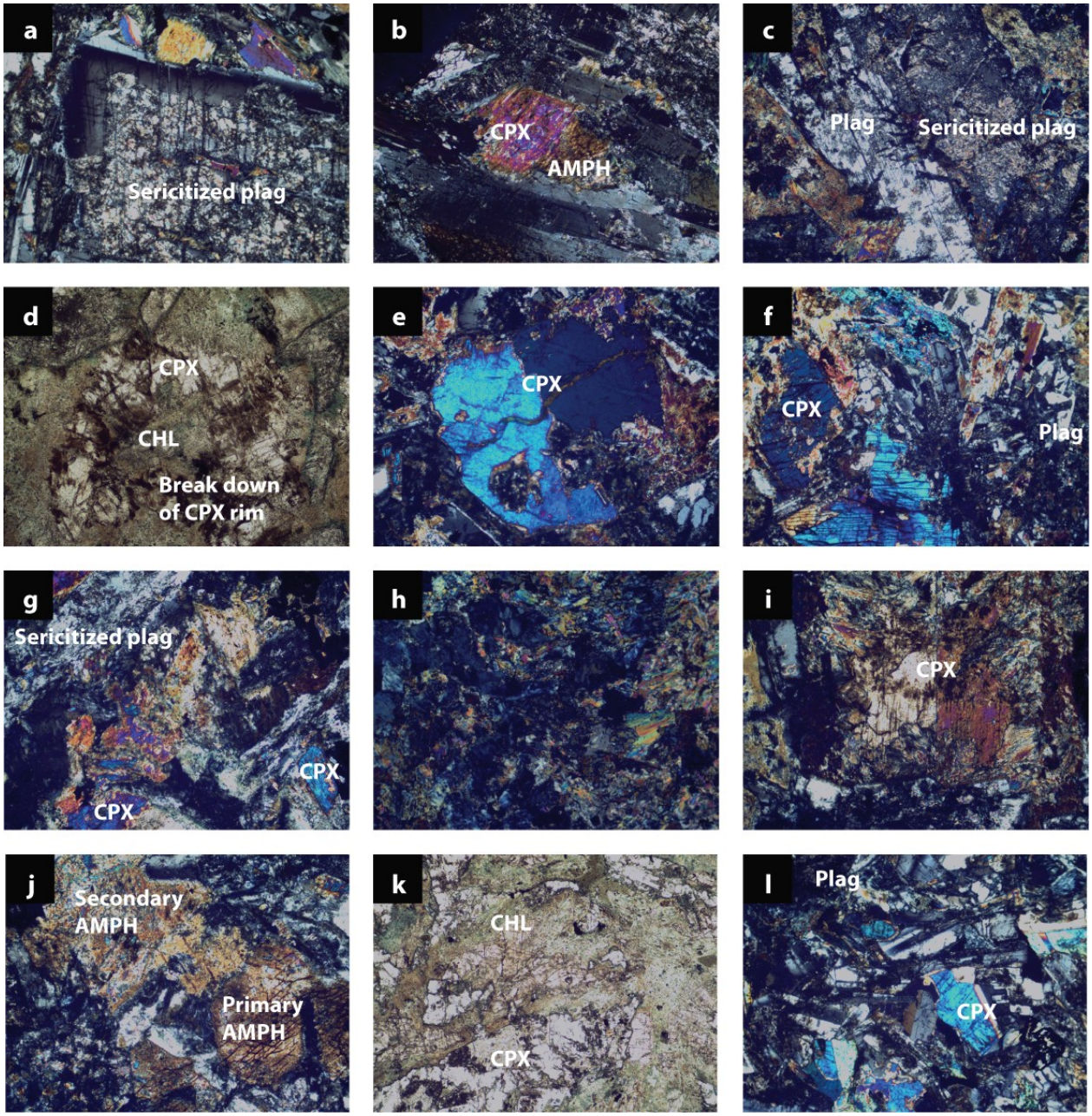

Fig. 8. a: A plagioclase phenocryst displaying sericitazion in the centre of the grain (JR03, crossed polars). b: A clinopyroxene grain partly replaced by amphibole on its right. The Fe-Mg minerals are surrounded by plagioclase (JR03, crossed polars). c: View of a plagioclase grain displaying typical sericitazion (JR06, crossed polars). d. This image shows the break down of clinopyroxene. The core is totally replaced by other minerals, i.e. chlorite, and the rim is starting to decompose (JR06, plane-polarized light). e. The clinopyroxenes display bright interference colours that change at the rims, presumably because of compositional zoning. This particular grain is starting to break down at the bottom right (JR07, crossed polars). f. Small plagioclase laths are surrounded by mafic minerals with an ophitic texture in this sample. The pyroxene at the bottom left show the same alteration as the one in b (JR07, Crossed polars). g. Clinopyroxene breaks down mainly to chlorite. The remnants of clinopyroxene displays compositional zoning close to the rims. Some sericitized plagioclase can also be seen (JR12, crossed polars). h. This whole picture shows a plagioclase phenocryst that is totally sericitized (JR12, crossed polars). i. A twinned clinopyroxene grain, which has started to break down (JR16, crossed polars). j. Primary amphibole in the bottom right with clinopyroxene breaking down to secondary amphibole in the top left. The small spots of bright blue interference colours are what are left of the pyroxene (JR16, crossed polars). k. A former clinopyroxene phenocryst which now is mainly replaced by chlorite (JR17, plane-polarized light). l. Picture showing the relatively fresh clinopyroxene grains with compositional zoning. Some of the grains show twinning. The plagioclase is partly sericitized (JR19, crossed polars). Abbreviations used in the photos are: Plag = plagioclase, CPX = clinopyroxene, AMPH = amphibole, CHL = chlorite

most other samples, only minor sericitazion was observed. Plagioclase is the most abundant mineral in the groundmass.

3.7 JR19 (S 26,648985° E 30,504398°)

This sample is collected far to the north of the previously described samples (approximately 180 km). It was taken in south-eastern Mpumalanga of South Africa. The dyke has negative relief, from where it intrudes the host rock of quartzite (Fig. 9). On fresh surfaces, it displays a medium-grain size, with only small and elongated feldspar crystals in a mafic groundmass. The dyke trends 025° NNE, and has intruded both the Usushwana Complex, and the overlying Mantonga quartzite at the base of the Pongola Supergroup.

Fig. 9: This dyke shows negative relief relative to the country rock into which it intrudes. The sample is taken from an in-situ boulder in the gully formed from the dyke intrusion. Photo taken by A. Gumsley.

In thin section, this is the best-preserved sample of all in the current study. Clinopyroxene is largely fresh, but shows some compositional zoning close to the rims. Plagioclase laths of different sizes are abundant and display only little sericitazion (Fig. 8l). Small grains of amphibole and chlorite are present, as are numerous small opaque minerals and a few quartz grains. The groundmass consists of plagioclase and small clinopyroxene grains together with a minor amount of quartz, chlorite and opaque minerals.

3.8 NED01 (S 28.210376° E 30.982430°)

This dyke is exposed in the Ntinini River, approximately 600 m upstream from where it merges with the White Mfolozi River. The contacts are not exposed, being covered by sand and water in the river's flood plain, which also makes the thickness of the dyke difficult to assess. The trend is 030° to the north-east, and only small scattered phenocrysts of plagioclase were noted in this diabase dyke. This dyke was drilled for paleomagnetic measurements, but no thin section was prepared of this sample.

3.9 BCD5-04 (S 26.646720° E 30.521970°)

This dyke was sampled and previously described by Olsson (2012), and the reader is referred to his paper for description. No thin section was made of this sample.

4 Methods, theory and analytical protocols

4.1 Geochronology

Baddeleyite is one of the last minerals to crystallize in a cooling silica undersaturated magma. It is found in the most fractionated parts of magma, i.e. in interstitial volumes between earlier-formed Ca-Fe-Mg minerals. The age of baddeleyite is therefore linked to the time of crystallisation of mafic rocks (Söderlund et al. 2013). Because of it's negligible initial Pb content in its crystal structure, and the high amount of U (several hundred ppm), baddeleyite is optimal for U-Pb geochronology (Heaman & LeCheminant 1993). Moreover, baddeleyite is sensitive to metamorphism at relatively low grades, and thus its presence indicated emplacement, not metamorphism, as it typically develops rims of polycrystalline zircon in the presence of free silica.

Baddeleyite extracted from fresh samples typically yields concordant to nearly concordant analyses. They might be up to 2 % discordant resulting from diffusional Pb loss near the crystal surface. Metamorphosed samples, however, often display frosty crystal surfaces made up of zircon. U-Pb dating of such composite grains will typically plot discordant for which the discordia will be a mixing line with end points depicted by the ages of the baddeleyite and zircon components, respectively.

4.1.1 Sample preparation

At the Department of Geology at Lund University, the rock samples were crushed to pea size using a hammer, before using a ring mill to crush it into a coarse powder. The powder was mixed with a drop of soap and water, and suspended before put on the Wifely Separation Table. Separation of baddeleyite was done according to the method of Söderlund & Johansson (2002). After separation, a magnetic pen was used to remove the magnetic minerals before baddeleyite grains were picked out under the microscope and transferred to a petri dish using a homemade plastic pipette.

For every sample, quality of the separated baddeleyites was compared, and the best crystals were combined into fractions of 1 to 6 crystals each, and put in separate pre-cleaned Teflon capsules. Every capsule went through a cleaning process containing several washing steps in ultra-clean 7N HNO_3 and H_2O. The capsules were then put on a hot plate for approximately one hour with a small quantity HNO_3 and H_2O, before the cleaning procedure was repeated. This procedure was done to limit the Pb blank in the samples before analysis.

After washing the Teflon capsule containing the cleaned baddeleyite grains, a spike solution which consisted of ^{205}Pb, ^{233}U and ^{236}U was added to every capsule together with ten drops of concentrated HF. The capsules were then placed for two days at 200°C in the oven to dissolve the baddeleyite and homogenizes the initial and spike U and Pb solutions.

At the Laboratory of Isotope Geology in the Museum of Natural History in Stockholm, the Teflon capsules were again put on a hot plate until the solution had evaporated completely. After adding ten drops of ultrapure 6N HCl to each capsule, one drop of 0.25 N H_3PO_4 was added to the samples before dried down on hotplate. The sample was re-dissolved in 2 µl Si-gel before loaded onto an out-gassed Re filament. The filaments were then heated until all the H_3PO_4 had burnt away and the sample turns white-grey on the Re filament.

4.1.2 Analysis

The analyses were done on a TIMS Finnigan Triton mass spectrometer at the Laboratory of Isotope Geology (LIG). The filaments were heated in a high vacuum chamber in the mass spectrometer and Pb isotopes were measured after heating to a temperature range of approximately 1200-1250°C. ^{204}Pb, ^{205}Pb, ^{206}Pb, ^{207}Pb and ^{208}Pb were measured in either static mode with Faraday Cups, or one at the time in peak-switching mode with a Secondary Electron Multiplier (SEM) amplifier. Large samples with strong and stable signals were preferably measured in static mode. The temperature was then increased to approximately 1270-1320°C where ^{235}U and ^{238}U isotopes were emitted and measured. An "in-house" program made by Per-Olof Persson (Natural History Museum, Stockholm) with calculations following Ludwig (2003) was used for data handling. TIMS data are presented in Table 1.

4.2 Geochemistry

The samples investigated in this study, and all relevant samples from the work of Olsson et al. (2010; 2011), were analysed for both major and trace elements. Samples in the JR series (03, 06, 07 and 17) were processed and analysed at the Central Analytical Facility (CAF) at the University of Stellenbosch, South Africa for major elements and trace elements. Major elements were analysed by X-Ray Fluorescence (XRF), using a Phillip's PW1404w instrument with 2,4 kW Rh X-Ray tube. Major elements were analysed on La-free fused glass beads and controlled by a range of international standards (NIST©). Trace elements were analysed from the same fused beads, using an Agilent 7500ce ICP-MS coupled with a Nd-YAG233 nm New Wave Laser Ablation (LA) system. It operated at a 12 Hz frequency, using a mixed He-Ar carrier gas. Each sampled was analysed with three spots (each 30 s blank followed by 60 s data collection), and an average was calculated. After three samples, standards were run.

Samples from the work of (Olsson et al. 2010; 2011) together with JR16, JR19, NED-01 and BCD5-04 were prepared for analysis at Lund University, Sweden. Rock samples were sawed and crushed with a sledge hammer into small pieces. The pieces were hand picked, in order to avoid phenocrysts of plagioclase and pieces with saw marks or weathered material. Diabase pieces were then milled in a tungsten carbide mill tray to a very fine powder. The mill tray was thoroughly cleaned with water and washing liquid, and dried between every sample. Approximately 10 g of each sample was sent to ACME laboratories in Canada for XRF (X-ray fluorescence spectrometry) analysis of major elements and ICP-MS analysis for trace elements. Loss on ignition (LOI) was also measured on every sample to determine the volatile content. The XRF analysis was done for major and minor elements on glass beads, which was prepared from the whole-rock powder. The sample-to-flux ratio was 1:10, and the precision was better than ± 1% of reported values. For the ICP-MS, samples were dissolved in 1.5 g lithium meta/tetraborate flux fusion. The resultant molten bead was rapidly digested in diluted nitric acid solution.

All XRF major elements and ICP-MS trace elements are presented in Table 2.

5 Results

5.1 Geochronology

Concordia diagrams illustrating the analyses are shown in Fig. 10 and analytical data from U-Pb TIMS dating is shown in Table 1. A total of seven samples were dated. Each dyke comprised between two and four analyses, and depending on size and quality of the baddeleyite grains, every analysis is made up of one to six crystals.

JR06

The grains are dark brown and of good quality, though many grains seem fractured. Two fractions made up of three and five grains respectively were prepared. The analyses plot slightly discordant (1-3.5%) and are partly overlapping. A weighted mean of $^{207}Pb/^{206}Pb$ yields an age of 2659 ± 5 Ma (MSWD = 1.8), which is interpreted to be the best age estimate of the dyke.

JR07

Two fractions of this sample were analysed comprising three and four grains. Grains are dark brown without any trace of zircon rims. Both analyses plot on the concordia allowing a concordia age to be calculated at 2664 ± 6 Ma (MSWD = 0.17).

JR16

Four fractions of good-quality grains were analysed. They consisted of one to four relatively light brown grains in each fraction. One fraction plots concordant at a younger age than the other analyses, resulting in a

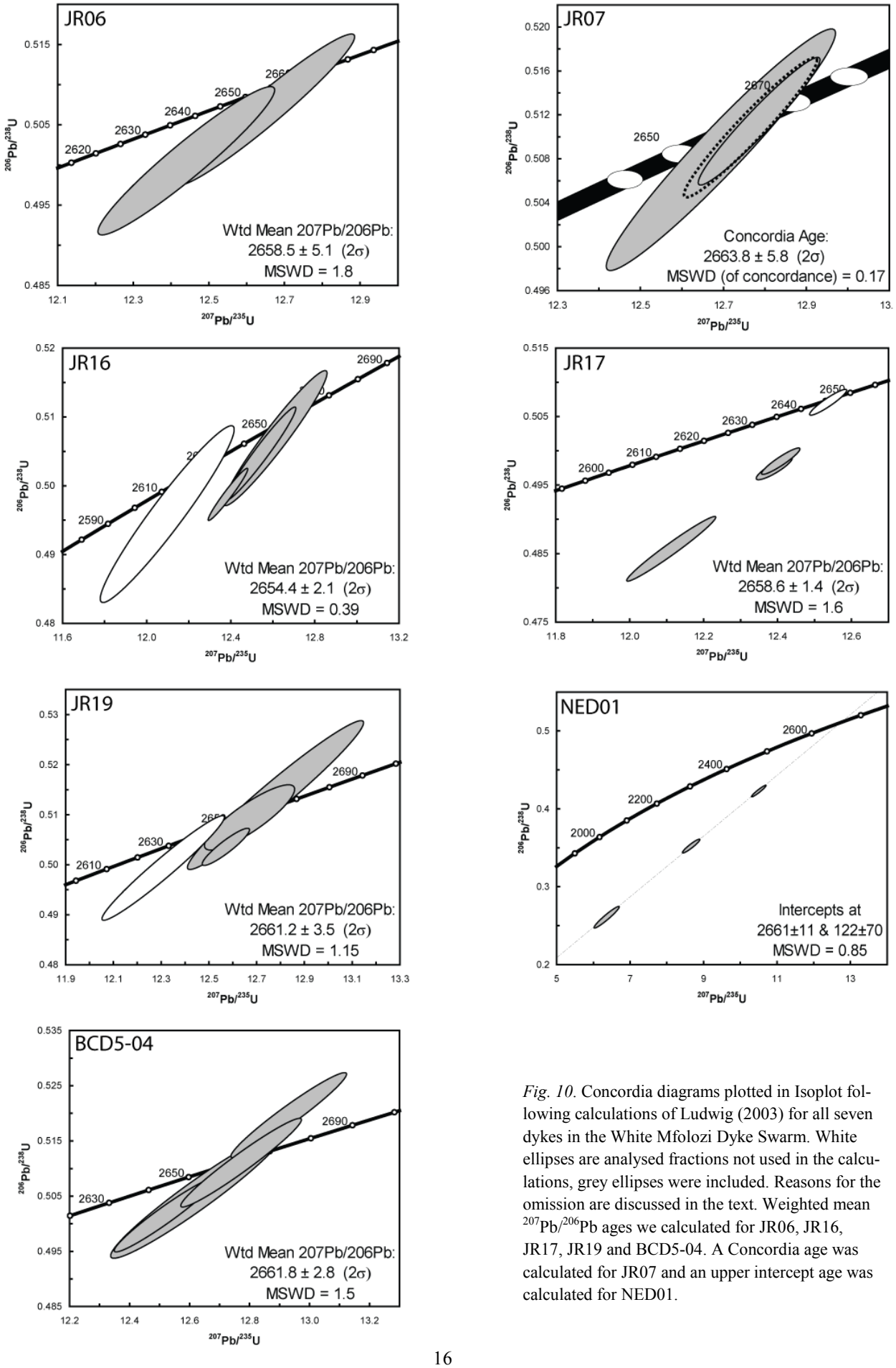

Fig. 10. Concordia diagrams plotted in Isoplot following calculations of Ludwig (2003) for all seven dykes in the White Mfolozi Dyke Swarm. White ellipses are analysed fractions not used in the calculations, grey ellipses were included. Reasons for the omission are discussed in the text. Weighted mean $^{207}Pb/^{206}Pb$ ages we calculated for JR06, JR16, JR17, JR19 and BCD5-04. A Concordia age was calculated for JR07 and an upper intercept age was calculated for NED01.

negative lower intercept age in the regression. 90 % of this sample (white error ellipse) was lost during mounting onto the Rhenium filament. Therefore, despite plotting concordant this analysis is omitted from age calculation. The other three ellipses overlap, and a free regression results in a lower intercept of 358 ± 820 Ma and an upper of 2657 ± 8 Ma. A weighted mean $^{207}Pb/^{206}Pb$ age gives a slightly younger and more precise result of 2654 ± 2 Ma. Two of the three fractions are concordant within error, and the third fraction is 2.1% discordant (MSWD = 0.39). The 2654 ± 2 Ma result is taken as the best estimate for the age of this dyke.

JR17

Four baddeleyite fractions of this sample were analysed. Brown-coloured transparent baddeleyite grains were combined into fractions of three to five grains each. Three fractions plot discordant (3-5%), and a weighted mean value yields a precise age of 2659 ± 2 Ma (MSWD=1.6). The fourth fraction is concordant, but plots at a lower age. If this fraction is included in the weighted mean, the upper intercept is 2655 ± 11 Ma, thus a less precise and slightly younger age. MSWD of 35 indicates scatter beyond analytical uncertainties, and therefore this analysis is rejected. The weighted mean of 2659 ± 2 Ma is interpreted as the age of this sample.

JR19

This sample, located close to BCD5-04, comprised analysis of four fractions, consisting of one to four grains. One analysis was performed on a single large, clear grain, while the other fractions consisted of three to four small grains of moderate to good quality. Three fractions overlap within error. Two of them plot con-

Table 1. U-Pb TIMS data for all analysed fractions.

Sample	Fraction (no. of grains)	U/ Th	Pbc/ Pbtot[1]	$^{206}Pb/^{204}Pb$ raw[2]	$^{207}Pb/^{235}U$ [corrected][3]	± 2σ % err	$^{206}Pb/^{238}U$ [corrected][3]	± 2σ % err	$^{207}Pb/^{235}U$ [age, Ma]	$^{206}Pb/^{238}U$ [age, Ma]	$^{207}Pb/^{206}Pb$ [age, Ma]	± 2σ (Ma)	Concordance
JR06	A (5)	6.2	0.151	362.0	12.4375	1.54	0.50059	1.50	2638.0	2616.3	2654.7	7.7	0.986
	B (3)	5.9	0.102	584.8	12.6469	1.53	0.50692	1.52	2653.7	2643.5	2661.5	6.8	0.993
JR07	A (4)	7.4	0.061	992.3	12.7874	0.94	0.51143	0.93	2664.1	2662.7	2665.2	4.3	0.999
	B (3)	n.m.[4]	0.281	198.8	12.6952	1.78	0.50883	1.77	2657.3	2651.6	2661.6	7.9	0.996
JR16	A (5)	7.2	0.037	1647.0	12.3847	0.62	0.49873	0.62	2634.0	2608.3	2653.8	2.6	0.983
	B (1)	8.3	0.128	460.5	12.6118	1.60	0.50694	1.58	2651.1	2643.6	2656.9	7.3	0.995
	C (2)	5.3	0.152	394.1	12.0950	2.16	0.49586	2.13	2611.8	2596.0	2624.1	10.4	0.989
	D (6)	8.1	0.078	776.6	12.5425	1.10	0.50467	1.10	2645.9	2633.8	2655.2	4.5	0.992
JR17	A (5)	13.1	0.066	793.4	12.3896	0.32	0.49747	0.28	2634.4	2602.9	2658.4	2.2	0.979
	B (3)	9.8	0.018	3182.3	12.4063	0.34	0.49847	0.32	2635.7	2607.2	2657.6	2.1	0.981
	C (5)	3.6	0.014	4208.2	12.5356	0.33	0.50710	0.31	2645.4	2644.2	2646.3	2.0	0.999
	D (3)	8.3	0.018	3221.9	12.1103	0.82	0.48564	0.80	2613.0	2551.8	2660.8	2.9	0.959
JR19	A (3)	6.1	0.248	185.4	12.6720	1.22	0.50949	1.05	2655.6	2654.5	2656.4	10.3	0.999
	B (1)	8.4	0.125	481.5	12.3094	1.71	0.49934	1.71	2628.3	2610.9	2641.7	6.9	0.988
	C (3)	5.5	0.149	417.1	12.7810	2.37	0.51395	2.37	2663.6	2673.5	2656.2	9.4	1.006
	D (4)	3.1	0.044	1246.0	12.5722	0.65	0.50356	0.60	2648.1	2629.1	2662.7	4.3	0.987
NED01	A (4)	7.9	0.394	108.8	8.6434	2.22	0.35206	2.10	2301.1	1944.4	2634.9	12.6	0.738
	B (3)	n.m.[4]	0.298	172.2	10.4950	1.53	0.42297	1.51	2479.5	2274.0	2652.5	7.5	0.857
	C (5)	2.1	0.485	90.7	6.3320	4.39	0.26027	4.33	2022.9	1491.2	2619.7	21.3	0.569
BCD5-04	A (2)[5]	5.3	0.186	270.8	12.8879	1.23	0.51883	1.22	2671.5	2694.2	2654.3	5.3	1.015
	B (3)[5]	7.4	0.196	253.7	12.5149	1.11	0.50136	1.10	2643.8	2619.6	2662.4	5.0	0.984
	C (3)	6.8	0.082	749.7	12.7736	1.29	0.51108	1.29	2663.1	2661.2	2664.5	6.8	0.999
	D (5)	5.1	0.189	285.3	12.6248	1.86	0.50506	1.84	2652.1	2635.5	2664.7	8.6	0.989

[1]) Pbc = common Pb; Pbtot = total Pb (radiogenic + blank + initial).

[2]) Measured ratio, corrected for fractionation and spike.

[3]) Isotopic ratios corrected for fractionation (0.1% per amu for Pb), spike contribution, blank (0.4-1.0 pg Pb and 0.04-0.1 pg U), and initial common Pb. Initial common Pb corrected w ith isotopic compositions from the model of Stacey and Kramers (1975) at the age of the sample.

[4]) n.m. = not measured

[5]) Data from Olsson el al. 2012

cordant. A weighted mean $^{207}Pb/^{206}Pb$ age of these three fractions is 2661 ± 4 Ma with a MSWD of 1.2. The fourth fraction plots concordant with a lower $^{207}Pb/^{206}Pb$ age of 2641.7 ± 6.9 Ma. Including this fraction in the weighted mean results yields a more imprecise result of 2657 ± 15 Ma, with a MSWD value of 9.3. Regression of the three grey ellipses yields an upper intercept age of 2657 ± 6 Ma, and a strongly negative and imprecise lower intercept age of -1367 ± 2900. Including the fourth fraction in a free regression yields a lower intercept age of 805 ± 3200 Ma and an upper intercept age of 2657 ± 28 Ma (MSWD = 3.7). The 2661 ± 4 Ma result is the preferred estimate for the age of this dyke.

NED01

Three fractions of three, four and five grains respectively were analysed. The grains show frosty surfaces. Analyses plot strongly discordant between 49 and 79%. A free regression yielded an upper intercept age of 2661 ± 11 Ma and a lower intercept age of 122 ± 70 Ma (MSWD = 0.85).

BCD5-04

Two fractions of this sample were analysed by Olsson (2012). Another two fractions composed of three and five grains each were analysed here. The baddeleyite grains selected for analysis are dark brown and clear. Some of them are elongated and some were fragments of presumably elongated crystals. One fraction plots concordant whereas the other fraction is 3.5% discordant. A regression made of all four analyses yield an age of 2662 ± 3 Ma. Using a forced lower intercept age at 0 ± 100 Ma gives an upper intercept that is identical if taken the weighted mean of $^{207}Pb/^{206}Pb$, i.e. 2662 ± 3 Ma (MSWD of 1.5)

5.2 Geochemistry

X-ray fluorescence (XRF) of major elements and inductively coupled mass spectrometry (ICP-MS) of trace elements are presented in Table 2. Fig. 11 shows that all dykes in this study are subalkaline. The White Mfolozi dykes plot in the centre of the basalt field together with the NE-trending 2660-2700 Ma dykes in the Mpumalanga and Limpopo provinces. The other coeval dykes of the Rykoppies swarm are all basaltic andesites. One sample from the outstanding Rykoppies dyke proper (BCD1-11), plots as an andesite. Therefore, except for one 2700 Ma NE-trending dyke, all basaltic dykes are around 2660 Ma, whereas all Ry-

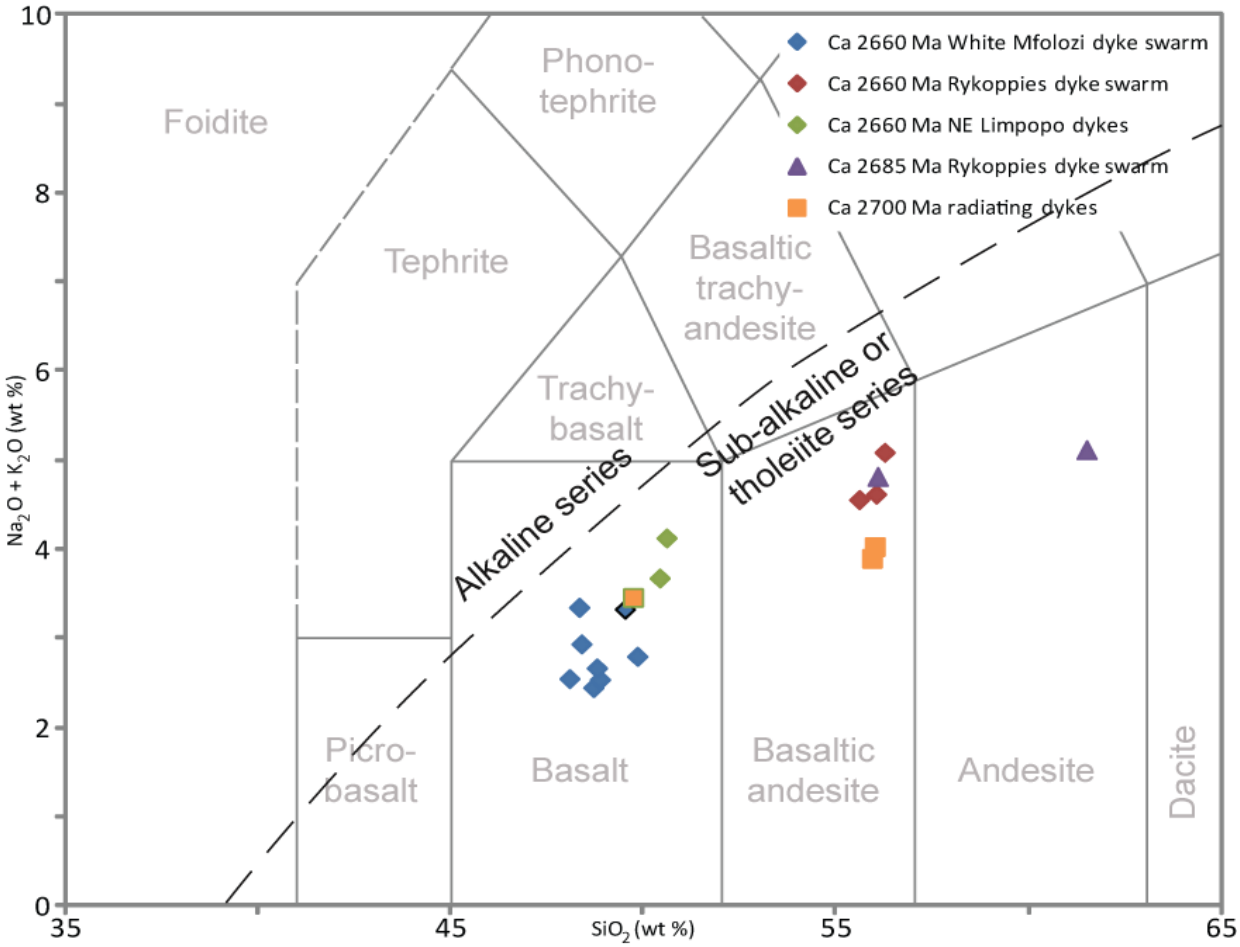

Fig. 11. All dykes are classified in the TAS plot after LeBas et al. (1986). Blue diamond with black margin is sample JR03. The orange square with green margin is BCD5-27. The dashed line are distinguishing alkaline from subalkaline dykes (Irvine & Baragar (1971).

Table 2. Major and trace element analyses on Neoarchaean dolerite dykes samples from the Kaapvaal Craton.

Sample	JR03	JR06	JR07	JR16	JR17	JR19	BCD5-04	NED01	BCD5-17	BCD5-18	BCD5-19	BCD5-22	BCD5-23	BCD1-09	BCD1-11[1]	BCD5-27	BCD3-08	BCD1-04
Trend (°)	15	48	23	27	23	25	NE	30	90	90	90	≈ 50	≈ 45	90	85	≈ 50	123	115
Age (Ma)	[4]	2659 ± 5	2664 ± 6	2654 ± 2	2659 ± 2	2661 ± 4	2662 ± 3	2661 ± 11	2662 ± 3[2]	2662 ± 3[2]	2659 ± 3[2]	2659 ± 13[3]	2662 ± 5[3]	2683 ± 2[2]	2686 ± 6[2]	2701 ± 11[3]	2692 ± 2[3]	2698 ± 4[3]
SiO_2	49.5	48.68	48.06	49.82	48.85	48.31	48.77	48.37	56.02	56.24	55.58	50.4	50.58	56.06	61.48	49.71	55.91	55.94
Al_2O_3	13.72	13.61	14.97	15.42	14.11	14.91	14.58	14.92	14.49	14.58	14.69	13.39	13.15	14.68	12.68	14.01	11.13	12.48
Fe_2O_3	14.97	14.74	12.93	11.46	13.41	13.28	12.73	13.11	9.21	9.19	9.56	16.59	16.63	9.09	8.17	15.2	10.65	10.74
MnO	0.21	0.22	0.2	0.18	0.2	0.19	0.19	0.19	0.12	0.13	0.13	0.21	0.2	0.13	0.1272	0.19	0.1536	0.171
MgO	4.94	5.93	6.46	7.06	6.63	6.67	7.23	6.95	4.81	4.67	4.82	4.71	4.28	4.84	4.62	5.25	9.49	6.33
CaO	8.88	9.77	10.69	10.01	10.42	9.42	10.43	9.52	8.26	7.27	8.05	8.93	8.22	7.82	6.56	9.22	7.13	8.9
Na_2O	2.59	2.1	2.13	2.21	2.34	2.74	2.26	2.29	3.37	3.58	3.48	2.63	2.65	3.49	3.3	2.47	2.8	2.65
K_2O	0.74	0.35	0.42	0.59	0.2	0.61	0.41	0.65	1.25	1.51	1.08	1.05	1.48	1.33	1.82	0.99	1.1	1.42
TiO_2	1.59	1.49	1.16	1	1.26	1.31	1.14	1.27	0.75	0.82	0.79	1.91	2.32	0.79	0.7016	1.65	0.7929	0.8619
P_2O_5	0.2	0.16	0.13	0.1	0.14	0.12	0.11	0.13	0.12	0.16	0.16	0.26	0.44	0.16	0.14	0.23	0.15	0.16
Cr_2O_3	0.01	0.02	0.03	0.033	0.03	0.032	0.036	0.04	0.014	0.024	0.017	0.009	0.012	0.025	0.0605	0.016	0.1562	0.0707
L.O.I.	1.42	1.5	1.69	1.8	1.61	2.2	1.9	2.3	1.3	1.6	1.4	-0.4	-0.3	1.3	1.36	0.8	0.89	1.46
TOTAL	98.77	98.57	98.87	99.68	99.20	99.79	99.79	99.74	99.71	99.77	99.76	99.69	99.66	99.72	101.02	99.74	100.35	101.18
Sc	34.95	40.64	35.53	36	39.81	33	35	36	22	21	23	39	34	21	12.88	35	16.68	20.4
V	307.06	312.98	258.30	234	284.83	246	231	303	165	170	160	324	276	155	107.60	293	160.22	187
Co	68.05	73.57	80.20	77.6	61.15	61.2	48.8	57.2	38.4	38.9	39.8	53.6	51.9	40.5	33.79	55	51.86	47.3
Ni	64.25	88.11	120.91	49	110.85	69.5	64.8	130	47.2	64.5	44.4	17.8	32.9	59.7	150.52	27.3	318.48	161
Cu	91.78	88.83	78.20	67.6	90.73	65.9	69.3	71.3	78.3	90.8	88.2	211	102.7	82.9	56.38	169.5	76.41	82
Zn	146.31	121.67	81.99	40	92.54	60	57	82	39	41	38	34	36	23	90.58	39	85.82	95
Rb	67.59	28.76	32.60	30	9.32	29.4	10.7	87	41.6	47.1	31.8	38.9	62.9	49	40.77	38.5	49.32	44.9
Sr	179.73	157.20	161.64	145	143.97	175	148.9	174.2	335.9	429.1	344.1	183.7	176.6	374.5	457.94	186	329.18	332
Y	31.62	29.64	22.75	19.2	24.59	23.6	22.6	25.1	15.6	19	17.3	40.3	51.5	20.6	15.79	35	15.70	16.6
Zr	116.37	89.93	68.68	57.6	73.52	77.3	71.1	78.1	110.7	133.2	123.7	197.8	285.9	131.9	143.95	167	126.62	125
Nb	5.45	3.91	3.05	2.2	3.25	2.9	2.9	3.5	4	4.2	3.8	10.6	16.6	4.2	5.95	8.8	5.43	5.05
Ba	215.84	66.37	46.89	99	36.89	106	80	119	371	500	360	238	343	375	375.74	202	262.08	303
La	11.50	5.86	4.34	3.7	4.76	6.6	5.6	5.2	17.5	20.5	19.4	21.3	32.7	20	24.23	18.2	19.01	17.97
Ce	26.02	15.15	11.35	9.5	12.26	14.6	13.4	13.1	35	40.1	38.2	48	74.3	39.8	50.75	40.8	41.39	39.5
Pr	3.45	2.26	1.75	1.48	1.89	2.13	2.06	2.02	4.25	4.86	4.76	6.21	9.17	4.68	5.56	5.28	4.63	4.59
Nd	16.12	11.99	8.81	7.6	9.39	10.9	10.1	9.8	16.1	21.4	19.7	27.7	39.1	18.1	20.58	23.5	18.01	18.32
Sm	4.36	3.58	2.79	2.03	2.75	2.7	2.8	2.93	3.06	3.81	3.68	5.89	7.83	3.84	4.11	5.13	3.85	3.92
Eu	1.46	1.29	1.05	0.9	1.10	1.08	1.1	1.13	1.04	1.29	1.14	1.75	2.15	1.23	1.27	1.57	1.18	1.3
Gd	5.19	4.48	3.48	2.9	3.78	3.9	3.66	3.66	3.4	3.94	3.53	6.53	8.43	4	3.92	5.71	3.81	3.95
Tb	0.90	0.74	0.61	0.52	0.63	0.66	0.65	0.67	0.55	0.57	0.59	1.17	1.48	0.62	0.53	1.02	0.52	0.54
Dy	5.83	5.31	4.26	3.47	4.45	3.8	4.05	4.22	2.9	3.33	3.35	6.95	8.65	3.2	3.11	5.94	3.10	3.27
Ho	1.19	1.13	0.86	0.81	0.95	0.86	0.96	0.96	0.57	0.71	0.68	1.46	1.83	0.63	0.58	1.26	0.57	0.61
Er	3.62	3.32	2.63	2.31	2.83	2.7	2.82	2.74	1.72	2.11	2.01	4.43	5.32	1.99	1.57	3.7	1.57	1.68
Tm	0.49	0.51	0.37	0.33	0.40	0.38	0.37	0.41	0.23	0.29	0.28	0.66	0.81	0.29	0.22	0.56	0.22	0.23
Yb	3.59	3.37	2.51	2.28	2.86	2.79	2.62	2.51	1.56	1.82	1.76	4.16	5.09	1.73	1.33	3.54	1.35	1.42
Lu	0.51	0.50	0.41	0.31	0.41	0.43	0.4	0.4	0.24	0.26	0.23	0.63	0.78	0.28	0.19	0.54	0.19	0.2
Hf	3.21	2.57	2.03	1.6	2.05	2.3	2	2.1	3.4	3.6	3.1	4.9	7.6	3.3	3.17	4.6	2.72	2.7
Ta	0.35	0.26	0.18	0.2	0.20	0.2	0.2	0.2	0.3	0.3	0.2	0.7	1.1	0.3	0.36	0.5	0.30	0.27
Pb	21.26	3.25	1.82	1.4	1.90	0.7	0.5	41.3	4.2	3.1	3.2	1.3	2.3	2	12.43	1.6	4.95	4.35
Th	1.45	0.45	0.30	0.2	0.32	0.6	0.5	0.3	2.5	2.4	2.5	2.9	4.2	2	2.89	2.6	2.41	1.83
U	0.28	0.12	0.09	<0.1	0.10	0.1	0.1	0.1	0.7	0.5	0.5	0.8	1.2	0.5	0.62	0.6	0.45	0.4
Mo	0.94	0.90	0.63	0.2	0.72	0.2	0.2	3.0	0.5	0.4	0.4	0.8	1.2	0.5		0.7		
Cs	1.89	1.09	1.79	2.4	0.67	1.4	1.2	1.1	1	0.7	0.5	1.4	3	2		2.2		

[1] BCD1-11 is the same dyke as BCD5-82
[2] Olsson et al. 2010
[3] Olsson et al. 2011
[4] Not dated

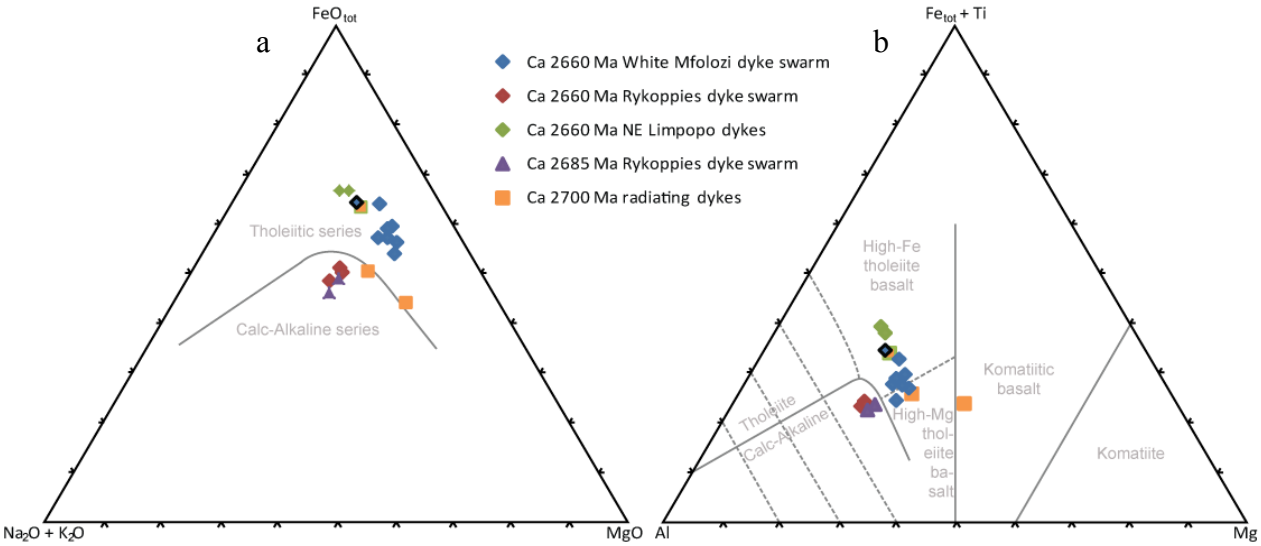

Fig. 12. Neoarchaean Kaapvaal Craton dykes plotted in (a) the AFM-diagram with the borderline after Irvine & Baragar (1971) and (b) the Jensen cation classification diagram by Jensen (1976). The diagrams clearly show that the WMDS has a tholeiitic character.

koppies dykes and older dykes are more evolved basaltic andesites and andesites.

Fig. 12a shows that basaltic dykes define a tholeiitic trend, whereas basaltic andesites and andesites (including all Rykoppies dykes) tend to be more borderline calc-alkaline. Dykes of the WMDS cluster around the border between Mg and Fe-rich tholeiitic basalts in Fig. 12b. Again, dykes of the Rykoppies swarm group together as calc-alkaline dykes regardless of being 2660 or 2685 Ma in age. It appears that at least one 2700 Ma basaltic is also relatively MgO-rich. Looking into the trace element geochemistry, the rare earth elements (REEs) display a distinct primitive flat character for the WMDS (Fig. 13). There is one sample, however, (JR03; blue diamond with black margin in previous plots, black-dashed blue line in upcoming plots) that has a more LREE enriched pattern than the other seven analysed samples in that swarm, yet not as LREE enriched as the Rykoppies and older dykes further to the north.

Also, the multi-element plot (Fig. 14) shows the significant difference between the WMDS and the other coeval sub-swarms on the Kaapvaal Craton. The WMDS is relatively low in Th, U, LREEs and Zr, ex-

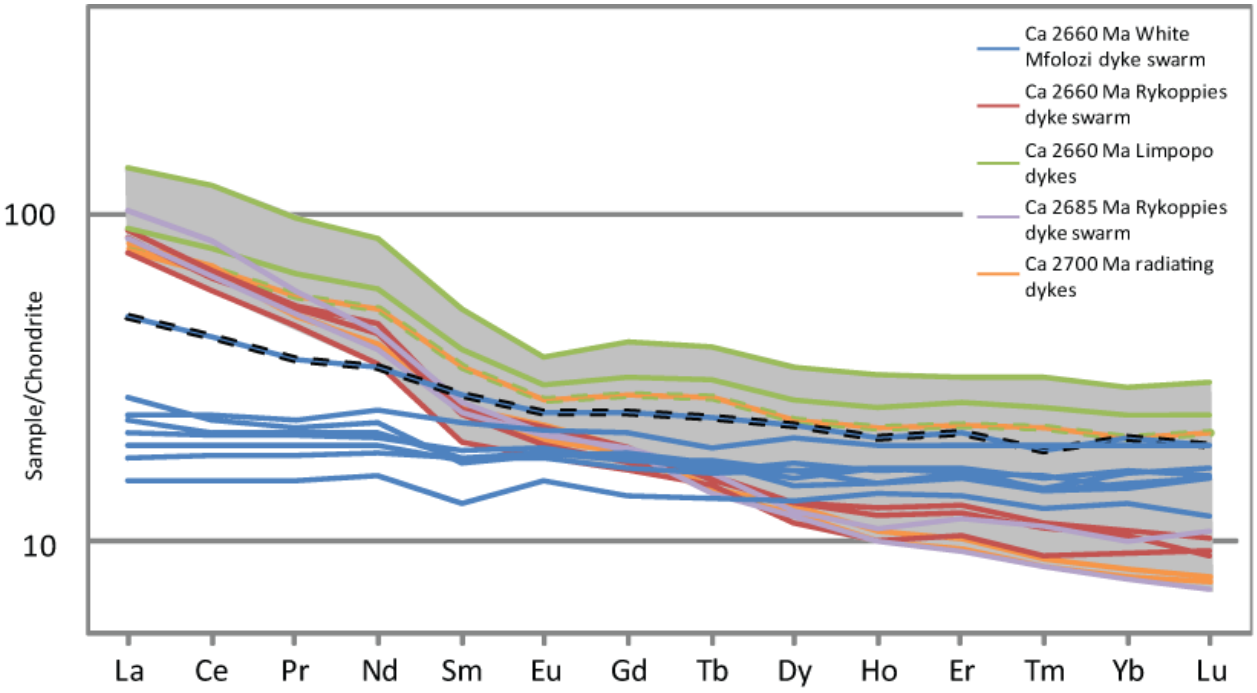

Fig. 13. The REEs are plotted on a variation diagram and normalized to the chondritic values of Sun & McDonough (1989). The grey-shaded area define the variation among the other dated Neoarchaean dyke swarms on the Kaapvaal Craton relevant to this study.

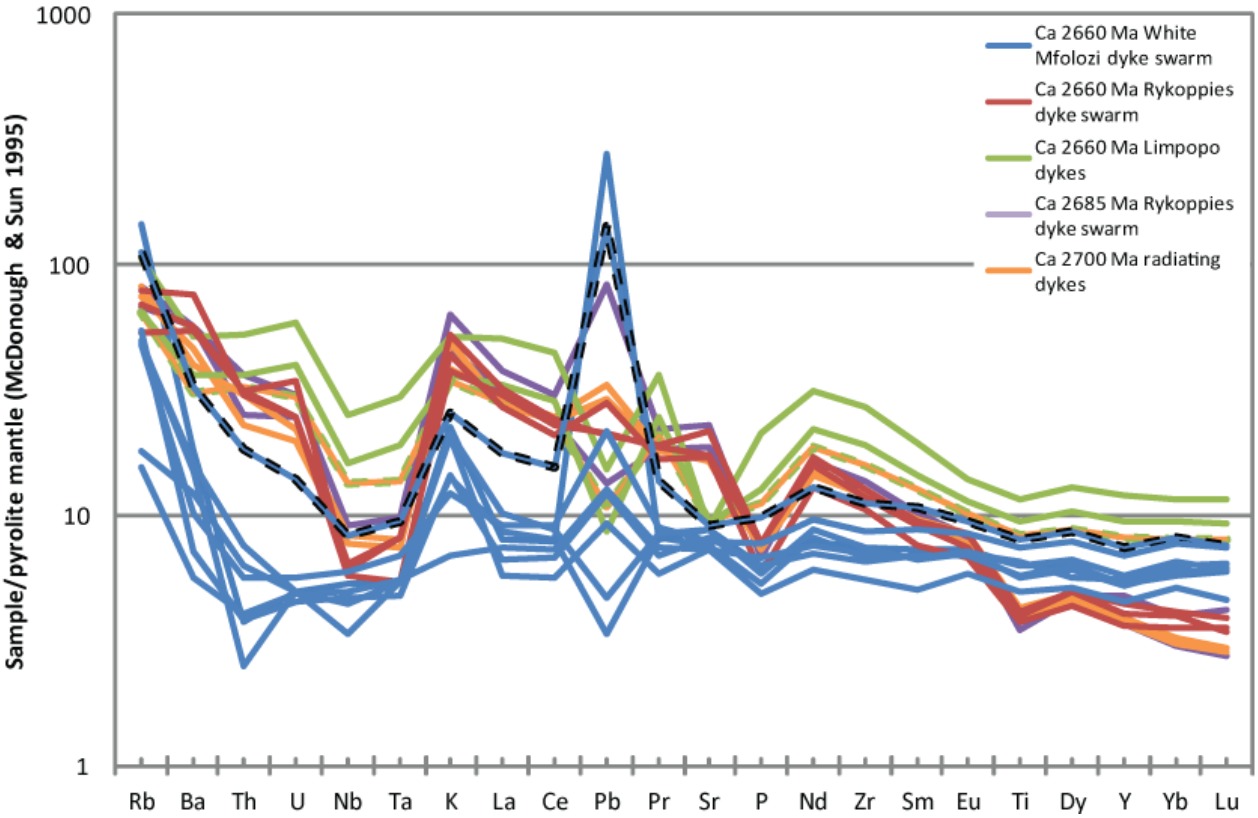

Fig. 14: Multi-element plot showing 19 elements of the samples normalized to pyrolite mantle (McDonough and Sun, 1995). The elements are shown from left to right, with increasing compatibility in a small fraction of mantle melt.

hibiting relatively low concentrations of the more incompatible elements compared to the less incompatible elements that characterize magmas derived from an enriched mantle. This results in much less pronounced Nb and Ta anomalies for the WMDS. The WMDS, nevertheless, still show some enrichment in Rb, K and Ba, compared to a more depleted pattern, as well as a remarkably large spread in Pb anomalies, which stretch over two orders of magnitude. Two of the more northerly located WMDS-dykes (JR19 & BCD5-04 from Mpumalanga) even show negative Pb anomalies, whereas NED01 and the southernmost sample JR03 stand out by having a strong positive Pb anomaly.

In comparison to the WMDS, the Rykoppies and older dykes all exhibit more enriched patterns. All of their patterns appear to be LILE/HFSE- and LREE-enriched, with negative Nb-Ta anomalies, an apparent subduction or contamination signature, yet a not very distinct Pb anomaly. Amongst these more evolved dykes, the Rykoppies dyke, and one of the radiating 2700 Ma dykes have relatively similar patterns that stand out by having lower HREE (possibly reflecting residual garnet in its mantle source), and negative P and Ti anomalies (possibly reflecting apatite and ilmenite fractionation, respectively). The two Limpopo dykes, and the other radiating 2700 Ma dyke have enriched patterns, with higher HREE and negative Sr-anomalies (indicative of plagioclase fractionation), yet with the Limpopo and radiating dykes having slightly different Pb anomalies.

6 Discussion

6.1 U-Pb data of analysed samples

Regression of three analyses of NED01 gives an upper intercept age of 2661 ± 11 Ma, similar to the mean age of ca. 2662 Ma for the White Mfolozi Dyke Swarm, despite all three analyses plot strongly discordant. The baddeleyite grains of this sample are frosty indicating post-magmatic metamorphism and/or alteration. The lower intercept of 122 ± 70 Ma implies zircon rims were formed during the ca. 180 Ma Karoo event, which is present in the area.

Free regressions of JR16, JR17 and JR19 yield negative or very imprecise lower intercept ages that include more or less all potential metamorphic events at which discordance could have developed, such as the ca. 180 Ma Karoo (Svensen et al. 2012) and the ca. 1.1 Ga Umkondo (Hanson et al. 2006) events. We chose to use weighted mean $^{207}Pb/^{206}Pb$ ages for all these three samples. This approach does not include any assumption as to when Pb loss occurred. On the other hand, the mean $^{207}Pb/^{206}Pb$ age only represents a minimum age if calculated from discordant analyses. However, in situations when discordance is only minor, the true emplacement ages can be inferred to fall within error of the mean $^{207}Pb/^{206}Pb$ dates.

Three of the four fractions (A, B and D) of JR16 overlap, of which two are concordant and within error. The concordant fraction C indicates a younger age. The low precision of this analysis is due to a loss

of ca. 90% of the sample during loading onto the Re filament. In this study this fraction is excluded from age calculation despite being concordant. When excluding this fraction, free regression yields an upper intercept age of 2657.1 ± 7.7 Ma, and an imprecise lower intercept age of 358 ± 820 Ma. Within error, it allows for discordance being linked to both the Karoo or the Umkondo magmatic events, or both. The weighted mean $^{207}Pb/^{206}Pb$ age of 2654 ± 2 (MSWD = 0.39) is therefore preferred as the minimum emplacement age of JR16.

The U-Pb data of JR19 is similar to JR16. Three fractions are overlapping, whereas a fourth fraction (B) plots concordant and within error but at a younger age. Adapting the same approach as for JR16, the three fractions yield an upper intercept age of 2657±6 Ma and a strongly negative and imprecise lower intercept age of -1367±2900. Including the fourth fraction in a free regression yields a lower intercept age (805±3200 Ma) that embraces all metamorphic events present in the area. This approach yields an imprecise upper intercept age of 2657 ± 28 Ma, and the MSWD of 3.7 reveals some scatter beyond analytical uncertainties alone. Thus, a weighted mean age of the three overlapping fractions is preferred, yielding a $^{207}Pb/^{206}Pb$ age of 2661 ± 3 Ma (MSWD = 1.1).

JR17 also displays one concordant fraction (C) of a slightly younger $^{207}Pb/^{206}Pb$ age relative the other three fractions. A free regression comprising the three more discordant analyses yields an upper intercept age of 2656±4 Ma, and a negative lower intercept age (MSWD = 0.27). The weighted mean of $^{207}Pb/^{206}Pb$ dates is 2659±4 Ma but with a slightly higher MSWD value of 1.6. Nevertheless, this is the preferred age of this sample though some uncertainty in this estimate is acknowledged due to discordant nature of analyses.
The two concordant fractions obtained for JR07 allow for a concordia age to be calculated. The result is 2664±6 Ma (MSWD = 0.17) and is interpreted as the age of crystallisation of the dyke.

We have chosen to also use weighted mean $^{207}Pb/^{206}Pb$ dates on the remaining samples JR06 and BCD5-04. They both display clustered analyses at or very close to the concordia, which means that a regression (anchored at 0 Ma), and a weighted mean age yields very similar emplacement ages. Due to the low degree of discordance for both of these samples, their respective results are interpreted as reliable crystallisation ages.

In this study, two analyses of BCD5-04 were performed, to complement the two pre-existing analysed fractions of BCD5-04 presented in Olsson (2012). Combining all four analysed fractions yields a weighted $^{207}Pb/^{206}Pb$ mean age of 2661.8±2.8 Ma. Considering the fact that three out of four fractions are concordant and within error, and the last fraction are almost concordant, this must be considered as a very robust age for this dyke located in southern Mpumalanga.

6.2 Timing and distribution of the White Mfolozi dyke swarm

The new U-Pb dating in this paper yield very similar emplacement ages for all dykes of the WMDS swarm indicating a very short duration of dyke emplacement. The three most robustly dated samples (JR07, JR19 and BCD5-04) have been chosen to represent a tentative "mean age" of the WMDS. A weighted mean of their emplacement ages including errors has been calculated to 2661.8 ± 2.0 Ma (MSWD = 0.3).

The swarm is characteristically feldspar-phyric and north-east trending. It can be found over a widespread area in northern KwaZulu-Natal and southern Mpumalanga. The dykes intrude basement rocks and old quartzites of Pongola Supergroup.

Sampled dykes that did not contain any baddeleyite, e.g. JR03 and JR12, may or may not be part of the same swarm as the dated dykes. They show similar trends and mineralogy. However, JR03 has a slightly different trend (015° N), and has a different chemical signature compared with the rest of the White Mfolozi dyke swarm (Fig. 14 and 15), indicating either significant contamination from the surrounding crust or a different magma source. Since there are no age data for this dyke, it cannot be ruled out that the dyke was emplaced by another event, though this is found unlikely. Like JR03, there are more dykes in Mhalutze River valley that have a more northerly trend than the WMDS. No baddeleyites have been found in any dyke from this region. JR12 also lacks geochemical data. The mineralogy and texture of JR03 and JR12 do not significantly differ from other dykes. However, these two samples are located close to the Natal Thrust Front on the edge of Kaapvaal Craton. The lack of baddeleyite may be explained by a stronger metamorphic imprint close to the thrust front, which may have replaced the baddeleyite with zircon. This is further supported by the observation that JR19, the sample furthest away from the thrust front is the freshest one. The Natal Thrust Front stem from orogenic events along the present-day southern margin of the Kaapvaal Craton at ca. 1,0 – 1,2 Ga (McCourt et al. 2006).

Fig. 16 shows a summary of all U-Pb results of this study, and compares them to age data published by (Olsson et al. 2010; 2011). It appears that concordant data sets (JR07, 19 and BCD5-04) yield slightly older ages (weighted mean 2661.8 ± 2.0 Ma) than most of the discordant data sets (JR06, 16, 17 and NED01). Considering emplacement ages constrained from weighted means of $^{207}Pb/^{206}Pb$ dates are minimum ages in a strict theoretical sense, one cannot rule out the possibility the true age of the sample is a few million years older.

If the concordant data sets represent the most robust emplacement age, whereas the true age of discordant sets are slightly older, then practically all dykes were emplaced in a shorter time interval than given by the their mean ages. In other words, the current U-Pb data do not preclude dykes of the WMDS

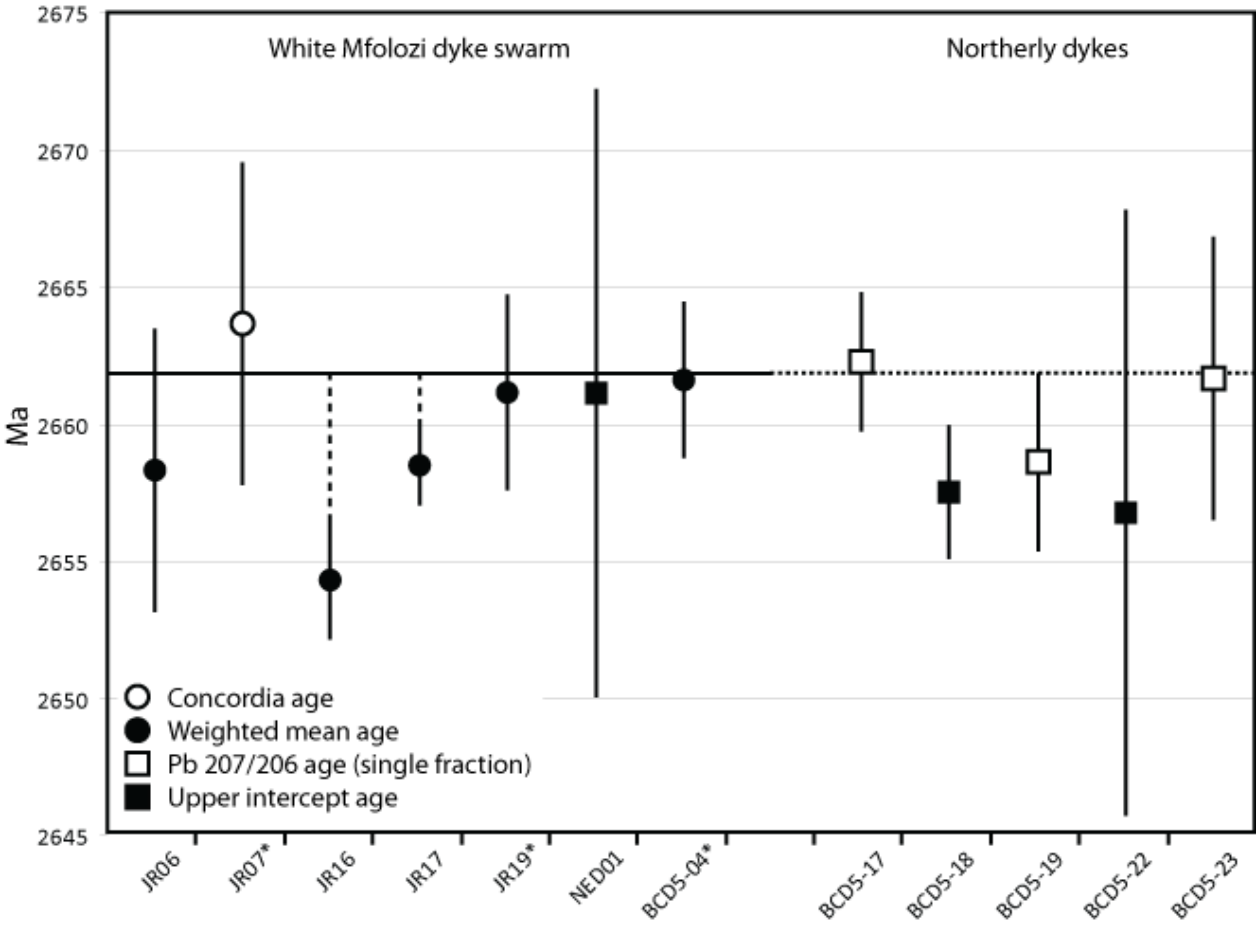

Fig. 15. All WMDS and five coeval dykes from further north (Olsson et al. 2010; 2011) are compared from a chronological perspective. The weighted mean ages from the three most "robustly dated" dykes (*) are drawn as a line at 2661.8 Ma. Dashed lines indicate that JR16 and JR17 might be a few million years older.

were emplaced within a very short time interval of 1 Myr, or less.

An event at approximately 2662 Ma would then be the best mean age of the WMDS. As is shown in Fig. 15, three E-W trending dykes (BCD5-17, 18 & 19) in northern Mpumalanga (>190 km north of BCD5-04), are identical in age (2659-2662 Ma; Olsson et al. 2010). Moreover, two NE-trending dykes (BCD5-22 and 23) further north in southern Limpopo (approximately 300 km north of BCD5-04) also are identical in age with the White Mfolozi Dyke Swarm, indicating that this event might have an even larger geographical area comprising a ca. 400 km wide dyke swarm (Fig. 18).

6.3 Three pulses of magmatism on the Kaapvaal craton

Considering all U-Pb baddeleyite ages of Neoarchaean dykes located along the eastern portion of the Kaapvaal Craton, including dykes of the NE-trending WMDS, the E-trending Rykoppies Swarm, the E-SE-trending Barberton-Badplaas Swarm and the NE-trending dykes in Limpopo, it seems like magmatism was episodic over a 40 Myr time interval, starting at approximately 2700 Myr ago.

Three pulses at ca. 2700 Ma, at ca. 2685 Ma and at ca. 2660 Ma, can be visually illustrated by plotting single fractions from sampled and dated dykes together in an U/Pb isotope diagram (Fig. 16).

The oldest magmatic pulse, comprising the ca. 2700 Ma dykes are plotted as brown ellipses (Fig. 16 and 17a) and are members of the proposed radiating swarm (Olsson et al. 2011) east of the Bushveld Complex, represented by the NE-trending dyke BCD5-27 and the SE-trending BCD3-08 and BCD1-04. BCD1-04 was earlier reported as 2672.9 ± 1.8 Ma by Olsson et al. (2010), but this age was constrained by a single fraction. The $^{207}Pb/^{206}Pb$ age of this analysis must be considered merely as a minimum age, because of its relatively strong discordance (5.5 %). The refined age result presented by Olsson et al. (2011) gave 2698.4 ± 3.6 Ma for this dyke, constrained by four moderately discordant analyses, which testifies this dyke belong to the oldest pulse. The probable cause of variability in discordance of baddeleyite from the same sample is presumably due to baddeleyite that is variably converted to zircon.

At ca. 2685 Ma, E-W-trending dykes were emplaced between the ca. 2700 Ma radiating dykes. They are plotted as blue ellipses (Fig. 16 and 17b) and represented by BCD1-09 and BCD5-82 (Olsson et al.

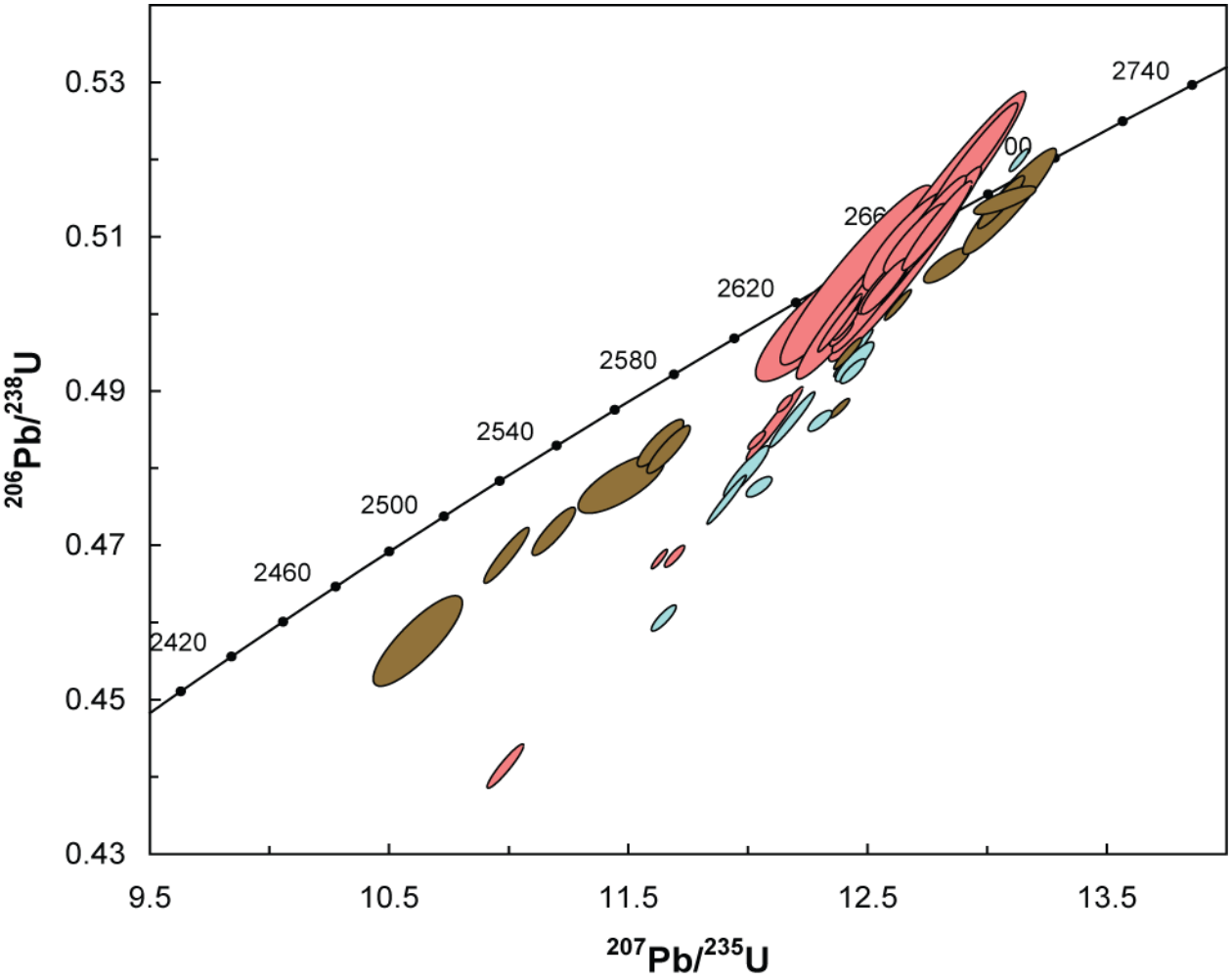

Fig. 16. All analysed fractions from the Kaapvaal Craton (this study, Olsson et al. 2010 & 2011) are plotted together to illustrate the three-pulse magmatism suggested in this thesis. Colours indicate approximate age of the dykes. Pink = 2660 Ma, blue = 2685 Ma and brown = 2700 Ma. Fig. 17 displays all fractions, sorted by age. NED01 consists of three fractions that are not displayed in this diagram for scale reasons. See Fig. 17c for their position on the U/Pb isotope plot.

2010). The ca. 2660 Ma White Mfolozi Dyke Swarm and coeval dykes in the Rykoppies Swarm (Olsson et al. 2010) and in Limpopo (Olsson et al. 2011) are plotted as pink ellipses (Fig. 16 and 17c) and represent the youngest pulse.

The ca. 2700 Ma swarm (brown ellipses) stand out in the way that it displays three distinguished trends of discordance in the concordia diagram with one main trend plotting along a line that intersects the concordia at ca. 1850 Ma. This is illustrated both in Fig. 16 and 17a. The fractions of BCD5-27 plot on or just below the reference line between 2.7 and 1.85 Ga. BCD5-27 is influenced by mixing between baddeleyite and polycrystalline zircon, developed at the time when the Black Hills swarm was emplaced at ca. 1.85 Ga (Olsson 2012). Mixing between baddeleyite and polycrystalline zircon leads to the ellipses ploting along the reference (mixing) line. The effect related to emplacement of the Black Hills Swarm can also be observed on the 2659 ± 13 Ma BCD5-22 sample in the same area as BCD5-27, as its lower emplacement age are close to 1.9 Ga, when using a free regression (Olsson et al. 2011). The two other dykes (BCD3-08 and BCD1-04) indicate younger discordance that developed at ca. 1000 and 0 Ma. They are located south of the Black Hills Swarm and show no effect of the ca. 1.9 Ga Black Hills event. The lower intercept age of 1018 ± 130 Ma for BCD1-04 indicates that this dyke was presumably affected by the ca. 1.1 Ga Umkondo event, and may have developed polycrystalline zircon at this time. The cause for the discordance of BCD3-08 probably relates to diffusional lead loss from baddeleyite in recent times, indicated by a lower degree of discordance and a lower intercept age close to 0 Ma.

The blue ellipses, representing the approximately 2685 Ma swarm stem from two E-trending dykes. Their lower intercepts do not overlap, even if they are only about 19 km apart in the Rykoppies Dyke Swarm.

The youngest ca. 2660 Ma pulse is represented by pink ellipses and comprise dated dykes in this paper, samples BCD5-17, BCD5-18 and BCD5-19 from Olsson et al. (2010), and samples BCD5-22 and BCD5-23 from Olsson et al. (2011). The reported age of BCD5-23 is 2674 ± 11 Ma. It is constrained by two

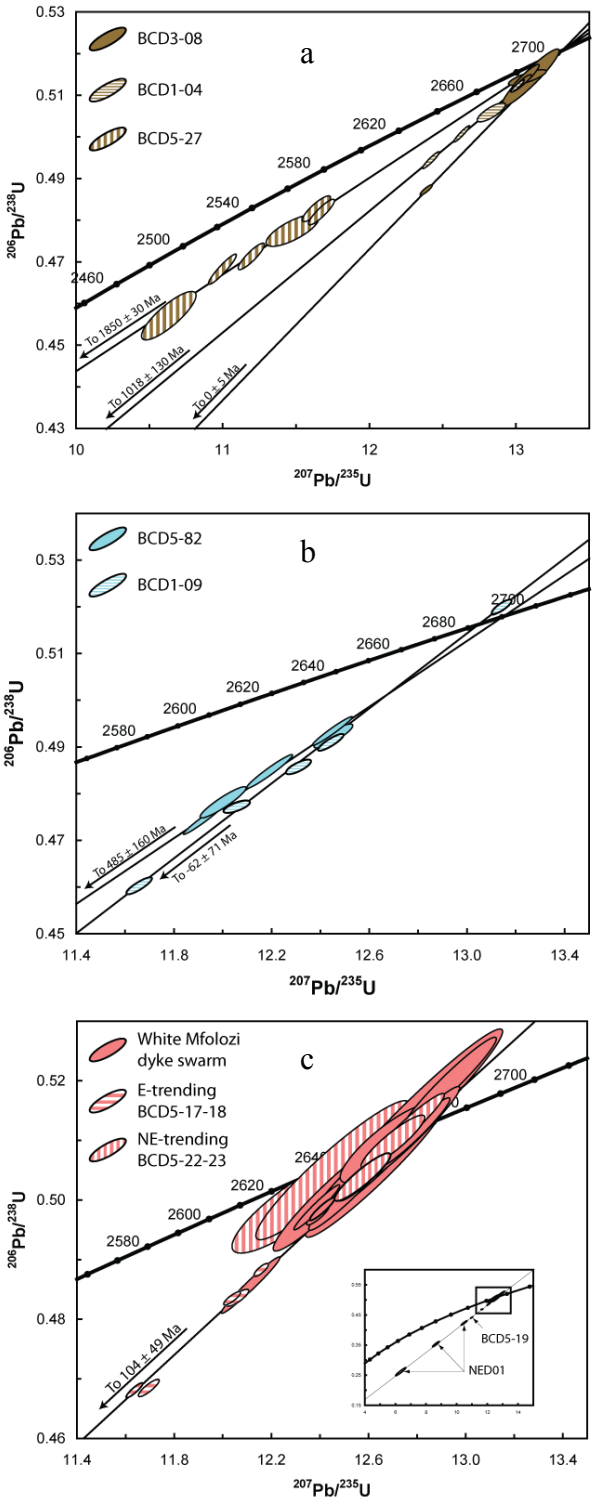

Fig. 17. The three generations from Fig. 16 are separated in order to identify the nature and timing of when discordance developed. Reference lines are included for clarity. (a) represents the oldest 2700 Ma generation, (b) the middle generation of E-trending 2685 Ma dykes and (c) consists of all dykes of the youngest ca. 2660 Ma generation. Note the pink sample NED01 that consists of three strongly discordant fractions plotting outside of both Fig. 16 and Fig. 17c.

fractions that plot far apart in the concordia diagram. I have chosen to use only the least discordant fraction (a, in Olsson et al. 2011) with a $^{207}Pb/^{206}Pb$ age of 2661.8 ± 5.1 Ma as a reliable minimum emplacement age for this sample. The reference line represents a regression made from all fractions (solid and striped) that are pink in Fig. 17c. The reference line intersects the concordia at the age of 2659.0 ± 2.4 Ma. This ca. 2660 Ma swarm consists mostly of NE-trending dykes except samples BCD5-17-19, which all have an easterly trend. The reason they diverge from a NE trend might be that they intruded into the crust where an earlier generation of E-trending dykes (the ca. 2685 Ma dykes of the Rykoppies swarm) already had been emplaced. Jourdan et al. (2006) argued that basement control might be a very powerful factor when younger dykes are to be emplaced, such that dykes may intrude along trends that deviate from the main stress direction. This may explain the presence of 2660 Ma dykes intermixed with older 2685 Ma dykes of the Rykoppies swarm. This is the only location where 2660 Ma dykes deviate from their normal NE trend. In the northern area, ca. 20 km west of the town Phalaborwa in the Limpopo province samples BCD5-22 and 23 intrude the bedrock in the same NE direction as the older BCD5-27 dyke. Satellite imagery over this area shows that dykes with a NE trend intrude the bedrock pervasively. Noteworthy is also that ca. 1.85 Ga dykes are intermixed with dykes of this swarm (Olsson, 2012). Hence, basement control and older zones of weakness might play an important role here as well. In northern KwaZulu-Natal, there are no (yet discovered) dyke swarms present which are older than ca. 2.7 Ga. This indicates that the NE trend of the White Mfolozi Dyke Swarm records the overall, and general stress direction (perpendicular to dyke trend) during the magmatic events.

6.4 Correlation with volcanic units on the Kaapvaal Craton

The spread in dyke ages of dykes from the Kaapvaal Craton (ca. 2660 – 2700 Ma) is coeval with the youngest rocks of the Venterdorp Supergroup, and its shift to the protobasinal fills of the Transvaal Supergroup. There are several ages of lava units in the Ventersdorp Supergroup (including proto-basin lavas), which could be correlated to the dykes here studied.

The north-east trend of many dykes on the Kaapvaal Craton during this time suggests a connection to Ventersdorp Supergroup, which was deposited in a series north-east trending graben structures (Uken & Watkeys, 1997). Ages obtained for different units in the middle of Ventersdorp stratigraphy reveals that these units are older than the oldest dated dykes on the craton. Armstrong et al. (1991) reports an age of 2709 ± 4 Ma for the Makwassie Quartz porphyry and slightly older 2714 ± 8 Ma for the underlying basalts of the Klipriviersberg Group. Both ages are obtained with U-Pb on zircon grains. The oldest age of the north-east

trending dykes on Kaapvaal Craton is reported by Olsson et al. (2011) from BCD5-27 at 2701 ± 11 Ma. This age overlap the Makwassie age within error. It cannot be ruled out that this dyke is part of a north-east Ventersdorp fabric. The north-east trending dykes cannot, however, be coupled to the oldest Ventersdorp. Younger dyking events like the second (ca. 2685 Ma) of the three pulses are possibly coupled to the younger Ventersdorp events. Olsson et al. (2010) proposed a possible correlation between the older (ca. 2685 Ma) Rykoppies dykes and the basaltic andesite lavas of the Allanridge formation (upper Ventersdorp Supergroup). This correlation is further strengthened by Klausen et al. (2010) and the chemical analysis of the Rykoppies dykes in this study, revealing that they are also basaltic andesites (Fig 11).

The ca. 2660 Ma White Mfolozi Dyke Swarm could most likely be correlated to the lavas in the protobasinal fill sequence at the bottom of Transvaal Supergroup, which are dated to 2657 - 2659 Ma (unpublished report, SACS 1993) and to 2664 Ma from U-Pb zircon (Barton et al. 1995).

6.5 Geochemistry of the White Mfolozi dyke swarm

The geochemical data clearly distinguishes the WMDS from other approximately 2.66 - 2.70 Ga old dykes on the Kaapvaal Craton. This restricts the WMDS to the south-eastern part of the Kaapvaal Craton. All studied dykes in this study are depleted basalt in chemical terms (Fig. 11), and are also characterized by having conspicuous feldspar megacrysts. However, due to their medium to coarse grained nature, they should rather be called microgabbros or diabases. Both the REE and multi-element diagrams (Fig. 13 and 14) show that the WMDS is of a characteristically more chemically depleted in character than other using chondrite and pyrolite mantle as a normative, unlike more northerly dykes. This is especially true in the more incompatible elements, like Zr, the LREEs and the LIL (Th, U and K), which are low for the WMDS. This signals that magma generating this swarm was chemically depleted, and its magmas could have been derived from a depleted mantle source, which received no or little crustal contamination during emplacement in the crust.

Within the White Mfolozi Dyke Swarm, there are some dykes that stand out. JR03, which were not dated as baddeleyite was absent, has a more enriched geochemical character, which is illustrated on both the REE and multi-element plots where it is marked with a black-dashed rim. This dyke plots in between the general REE compositions of the WMDS and the other more enriched dykes further north (Fig. 13). Possible explanations include that JR03 is either more extensively crustally contaminated, or that this dyke has a different origin and is of a different age. Because of the lack of age data from this dyke, it is impossible to rule out the latter explanation, but the feldspar phenocrysts give good reason to believe that it is part of the WMDS. The two White Mfolozi dykes located in Mpumpalanga (JR19 and BCD5-4, Fig. 2) have a negative Pb anomaly (Fig. 14), which, together with their northern location, separates them from the other dykes in the JR-series. Large variations of Pb concentrations are not uncommon due to the high mobility of the divalent Pb ion however.

6.6 Geochemistry of other Neoarchaean Kaapvaal dyke swarms

6.6.1 Rykoppies swarm

Dykes of the Rykoppies swarm consist of two well-established age groups of approximately 2660 and 2685 Ma in age. Those samples are geochemically calc-alkaline rocks (Fig. 13). However, one of the older dykes (BCD1-11) has dramatically higher SiO2 content, making it andesitic while the rest of the samples are classified as basaltic andesites. The REE and trace element geochemistry are both very consistent among dykes of the Rykoppies swarm, with no apparent differences with respect to age, suggesting that they have a common or similar source, or are all strongly affected by crustal contamination. The Rykoppies dyke BCD1-11 is rich in xenoliths, which support that the crustal contamination may dominate the geochemical signatures of the Rykoppies dykes (Klausen et al. 2010).

6.6.2 Limpopo dykes and radiating dykes

The northerly dykes in the Limpopo Province also show a distinct geochemical similarity to each other, despite the large age span of ca. 40 Myr between 2659 and 2701 Ma. The dykes have similar trends but the age span suggests that they might have been emplaced by different mechanisms. Pre-intrusive zones of weakness in the basement may have controlled the direction of younger dykes, as is already noted. Also for these dykes, the host rock seems to have had a big impact on their common geochemistry. The oldest, NE-trending Limpopo Dyke sample (BCD5-27, 2701 ± 11Ma) does not appear to have any geochemical similarity to the coeval SE trending dykes further to the south. In the geochemical diagrams, they are grouped together as the ca. 2700 Ma radiating swarm, but BCD5-27 is marked with green border/dashes to indicate its similarity to the younger NE-trending Limpopo Dykes. Still, BCD5-27, BCD1-04 and BCD3-08 might be members of a radiating swarm at 2700 Ma.

6.7 Contradicting the 40 Ma radiating swarm?

Olsson et al. (2011) proposed a radiating swarm that originated from a mantle plume impact where the eastern lobe of Bushveld complex is located today at approximately 2700 Ma. The authors attribute all radiating 2,66-2,70 Ga dykes on the Kaapvaal Craton to this plume event, despite an apparent large age span of ca. 40 Myr. Considering that the WMDS has been robust-

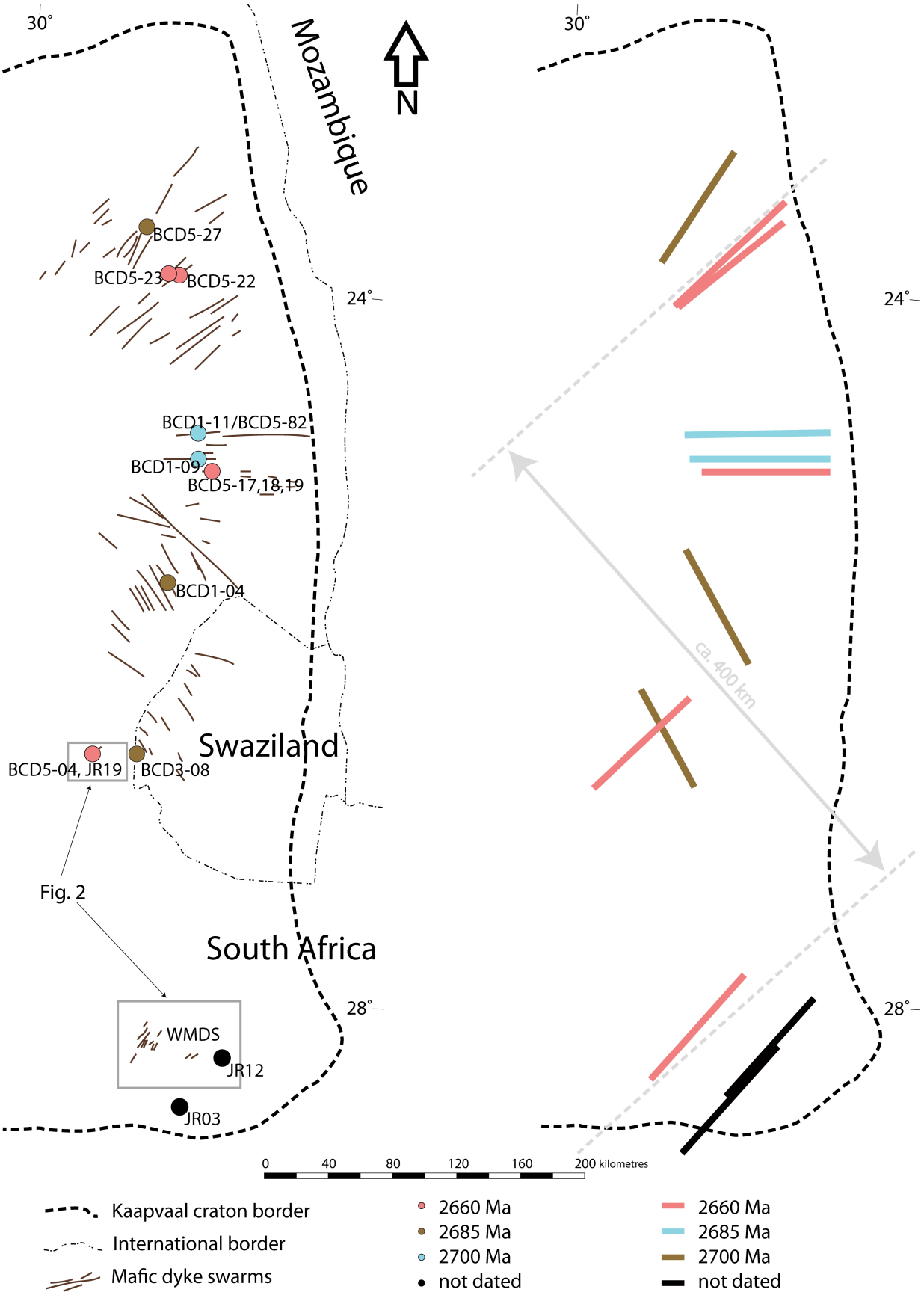

Fig. 18. This map (modified from Frick (1997)) shows the distribution of dykes along the eastern Kaapvaal Craton. The White Mfolozi Dyke Swarm is located within the two grey boxes (see Fig. 2 for detailed maps and exact sample sites). Given ages are approximate, see Fig. 10 for precise ages of the dykes. To the right, the dykes are exaggerated for clarity. The width of the dyke swarm is approximately 400 km and even wider if JR03 and JR12 are included in the WMDS.

ly dated and investigated geochemically, the duration of dyking related to a mantle plume must be reconsidered.

From their location (Fig. 18), the NE-trending dykes of the White Mfolozi Dyke Swarm in Mpumalanga appear to crosscut the SE-trending branch of the proposed 2.70-2.66 Ga radiating dyke swarm in Olsson et al. (2011), even though it has not been observed in outcrop. The sample site for NE-trending JR19 and BCD5-04 are only ca. 32 km west of the SE-trending BCD3-08. If those three dykes are stretched 20-30 km along strike northward, the NE dykes will crosscut the SE dyke, which according to Olsson et al. (2011) is part of the radiating swarm. The proposed radiating swarm are emplaced over a time span of 40 Ma, which contradicts a short-lived mantle-plume event.

The new age data of the White Mfolozi Dyke Swarm, together with age matching further north (Fig. 15) indicates a separate event being responsible for the emplacement of all ca. 2660 Ma NE- and E-trending dykes. This would limit the radiating swarm of Olsson et al. (2011) to maximum 15 Myr (approximately 2700-2685 Ma). However, geochemical data from ca. 2662 Ma dykes deviate. The White Mfolozi Dyke Swarm displays a primitive REE pattern, while the ca. 2660 Ma dykes further north and JR03 display a slightly LREE-enriched pattern, in accordance with older dykes in the radiating swarm. Moreover, none of the dykes outside White Mfolozi dyke swarm contain the characteristic feldspar megacrysts. This causes doubt over a common source for all ca. 2660 Ma dykes. One possibility is that a common mantle source was increasingly contaminated further north, deeper into the cratonic hinterland. This can be explained by thinner continental crust in the southern region, which is closer to the craton margin. If this is true, a more extensive crustal contamination affected the northerly dykes. The dyke geochemistry is then to a large extent dependent on contamination from the host rock which they intruded and the dyke swarm is approximately 400 km wide (Fig. 18).

Also supporting a model where the WMDS is derived from a more primitive source while the other dykes are more contaminated is the Th/Ta-La/Yb plot (Fig. 19). All WMDS samples plot on the lower left of the diagram, where the ratios of depleted and primitive mantle are present. Overall, all other dykes plot along the mixing line between upper continental crust and the primitive mantle. However, if they have been evolved along the hypothetical mixing curve of WMDS, they might have a depleted mantle source. Slight differences between different subgroups with slightly different multi-element patterns in Fig. 14 might be attributed to slightly different types of crustal contaminants in areas of the Kaapvaal Craton. The hypothetical mixing line drawn in Fig. 19 might be valid for all dykes. The northern dykes might be derived from the same magma source, but their magma is more evolved along this mixing line, indicating increasing contamination by a thicker crust further north.

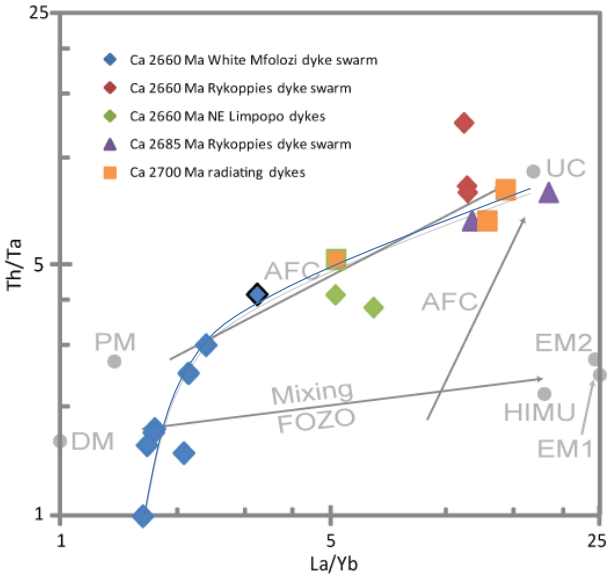

Fig. 19. Th/Ta plotted versus La/Yb. DM=depleted mantle; PM=primitive mantle; FOZO=focal zone mantle; EM1 and EM2=enriched mantle sources; HIMU=high-mu source; UC=upper continental crust; AFC=assimilation-fractional crystallization trajectory. A hypothetical mixing curve is drawn in blue for the WMDS.

The north-eastern trend of the dykes stem from the general stress direction which was acting on the Kaapvaal Craton during deposition of Ventersdorp Supergroup. Rifting was going on at ca. 2660 Ma, like Stanistreet & McCarthy (1991) proposed. The cause for rifting is not solved by this work, nor is the extent of the WMDS. Further work will be needed to clarify their emplacement mechanisms and to which extent these NE-trending dykes belong to one or more swarms.

7 Conclusions

- In the south-easternmost basement window on the Kaapvaal Craton, a swarm of north-east trending diabase dykes intruded the bedrock at approximately 2662 Ma. This swarm are characteristically feldspar phyric and shows a depleted geochemical signature. Most of the samples come from outcrops in and around the valley of the White Mfolozi River, and the name: White Mfolozi Dyke Swarm (WMDS) is proposed for this swarm. The dykes are all moderately metamorphosed, some more so than others. The degree of alteration is generally increasing towards the south, where they are close to the Natal Thrust Belt.
- The swarm spans over an area at least 190 km from north to south and 40 km perpendicular to this trend. However, if the coeval and NE-trending dykes in Limpopo are part of the same swarm, it is a major swarm, with a width of almost 400 km. The WMDS appear to crosscut the SE trending branch of the 2660-2700 Ma radiating swarm further to the north, even

though it is not observed in outcrops.

- Coeval dykes occur further north, in the South African provinces of Mpumalanga and Limpopo. They are the NE and E trending branches of the radiating swarm of this age, but they lack feldspar phenocrysts. Both of the branches contain dykes of approximately 2660 Ma, and a generation of slightly older dykes. The 2660 Ma dykes might be emplaced along previous zones of weakness attributed to reactivation of tectonic zones of weakness.
- The geochemical signatures for the northernmost ca. 2.66 Ga dykes differ from the coeval WMDS. They dykes in the north are more enriched, indicating more extensive crustal contamination or a shallower mantle source than for WMDS. There are two possibilities: one is that all dykes were derived from a chemically similar mantle source. It would be a depleted source and the magma would have been more evolved the further north it intruded the bedrock. The other option is that there were two simultaneous events going on, with two chemically distinct magma sources, and that crustal contamination was limited in both areas.

8 Acknowledgments

First of all, many big thanks to my supervisor, Professor Ulf Söderlund and my co-supervisor Ashley Gumsley, for giving me the opportunity to do this project! Ulf, thank you for all your time spent on reviewing my thesis, discussing and helping me through out this time. Ashley, thank you for making this project possible by taking me on a great field trip to the South African wilderness. I am very grateful for that, an I will remember it for the rest of my life! Thanks also for all hours you have spent on answering my questions, helping me with figures and discussing my results. My second co-supervisor, Dr. Martin B. Klausen, thank you for your participation in field and for all help and discussions via e-mail on the geochemical part of this thesis.

9 References

Anhaeusser, C. R. 2006. Ultramafic and Mafic Intru sions of the Kaapvaal Craton. In: Johnson, M. R., Anhaeusser, C. R. & Thomas, R. J. (eds.) The Geology of South Africa. pp. 95-134: The Geological Society of South Africa, Council for Geoscience.

Armstrong, R. A., Compston, W., Retief, E. A., Wil liams, I. S. & Welke, H. J. 1991. Zircon ion microprobe studies bearing on the age and evo lution of the Witwatersrand triad. Precambrian Research, 53, 243-266.

Barton, J. M., Blignaut, E., Salnikova, E. B. & Kotov, A. B. 1995. The stratigraphical position of the Buffelsfontein Group based on field relation ships and chemical and geochronological data. South African Journal of Geology, 98, 386-392.

Beukes, N. J. & Cairncross, B. 1991. A lithostrati graphic-sedimentological reference profile for the Late Archaean Mozaan Group, Pongola Sequence: application to sequence stratigraphy and correlation with the Witwatersrand Super group. South African Journal of Geology, 94, 44-69.

Beukes, N.J. & Gutzmer, J. 2008. Origin and Pa laeo environmental significance of major iron for mations at the Archaean-Palaeoproterozoic boundary. In: Hagemann, S., Rosiére, C., Gutz mer, J. & Beukes, N.J. (eds) Banded Iron For mation-related high-grade iron ore. pp 5-47: Reviews in Economic Geology, v.15

Bleeker, W. 2003. The late Archean record: a puzzle in ca. 35 pieces. Lithos, 71, 99-134.

Bleeker, W. & Ernst, R. 2006. Short-lived mantle gen erated magmatic events and their dyke swarms: The key unlocking Earth's palaeogeographic record back to 2.6 Ga, London, Taylor & Fran cis Ltd, 3-26

Bradley, D. C. 2011. Secular trends in the geologic record and the supercontinent cycle. Earth-Science Reviews, 108, 16-33.

Brandl, G., Cloete, M. & Anhausser, C.R. 2006. Ar chaean Greenstone Belts. In: Johnson, M. R., Anhaeusser, C. R. & Thomas, R. J. (eds.) The Geology of South Africa. pp. 9-56: The Geo logical Society of South Africa, Council for Geoscience.

Cawthorn, R. G., Eales, H. V., Walraven, F., Uken, R. & Watkeys, M. K. 2006. The Bushveld Com plex. In: Johnson, M. R., Anhaeusser, C. R. & Thomas, R. J. (eds.) The Geology of South Af rica. pp. 261-281: Geological Society of South Africa/Council for Geoscience.

Cheney, E. S. 1996. Sequence stratigraphy and plate tectonic significance of the Transvaal success sion of southern Africa and its equivalent in Western Australia. Precambrian Research, 79, 3-24.

Coffin, M. F. & Eldholm, O. 1994. Large Igneous Provinces: Crustal Structure, Dimensions, And External Consequences. Reviews of Geophys ics, 32, 1-36.

Cole, E.G. 1994. Lithostratigrapyh and depositional environment of the Archaean Nsuze Group, Pongola Supergroup. M.Sc thesis (unpublished). Rand Afrikaans University, Johannesburg, South Africa. 166 pp.

Cornell, D. H., Schütte, S. S. & Eglington, B. L. 1996. The Ongeluk basaltic andesite formation in Griqualand West, South Africa: submarine al teration in a 2222 Ma proterozoic sea. Precam brian Research, 79, 101-123.

de Kock, M. O., Beukes, N. J. & Armstrong, R. A. 2012. New SHRIMP U–Pb zircon ages from the Hartswater Group, South Africa: Implica

tions for correlations of the Neoarchean Vent ersdorp Supergroup on the Kaapvaal craton and with the Fortescue Group on the Pilbara craton. Precambrian Research, 204-205, 66-74.

De Wit, M. J., Roering, C., Hart, R. J., Armstrong, R. A., Deronde, C. E. J., Green, R. W. E., Tre doux, M., Peberdy, E. & Hart, R. A. 1992. For mation Of An Archaean Continent. Nature, 357, 553-562.

Duncan, A. R. & Marsh, J. S. 2006. The Karoo Igne ous Province. In: Johnson, M. R., Anhaeusser, C. R. & Thomas, R. J. (eds.) The Geology of South Africa. pp. 501-: The Geological Society of South Africa, Council for Geoscience.

Eglington, B. M. & Armstrong, R. A. 2004. The Kaap vaal Craton and adjacent orogens, southern Africa: a geochronological database and over view of the geological development of the cra ton. South African Journal of Geology, 107, 13-32.

Eriksson, P. G., Altermann, W., Catuneanu, O., van der Merwe, R. & Bumby, A. J. 2001. Major influences on the evolution of the 2.67-2.1 Ga Transvaal basin, Kaapvaal craton. Sedimentary Geology, 141-142, 205-231.

Eriksson, P. G., Condie, K. C., Westhuizen, W. v. d., Merwe, R. v. d., Bruiyn, H. d., Nelson, D. R., Altermann, W., Catuneanu, O., Bumby, A. J., Lindsay, J. & Cunningham, M. J. 2002. Late Archaean superplume events: a Kaapvaal-Pil bara perspective. Journal of Geodynamics, 34, 207-247.

Ernst, R. E., Wingate, M. T. D., Buchan, K. L. & Li, Z. X. 2008. Global record of 1600-700 Ma Large Igneous Provinces (LIPs): Implications for the reconstruction of the proposed Nuna (Columbia) and Rodinia supercontinents. Pre cambrian Research, 160, 159-178.

Frick, C. 1997. 1:1 000 000 Geological Map of the Republic of South Africa and the Kingdoms of Lesotho and Swaziland. Council for geoscience.

Gold, D. J. C. 2006. The Pongola Supergroup. In: John son, M. R., Anhaeusser, C. R. & Thomas, R. J. (eds.) The Geology of South Africa. pp. 135-147: The Geological Society of South Africa, Council for Geoscience.

Gumsley, A. P., de Kock, M. O., Rajesh, H. M., Knop er, M. W., Söderlund, U. & Ernst, R. E. 2013. The Hlagothi Complex: The identification of fragments from a Mesoarchaean large igne ous province on the Kaapvaal Craton. Lithos, 174, 333-348.

Hanson, R. E., Gose, W. A., Crowley, J. L., Ramezani, J., Bowring, S. A., Pancake, J. A. & Mukwak wami, J. 2004. Paleoproterozoic intraplate mag matism and basin development on the Kaapvaal Craton: Age, paleomagnetism and geochemistry of ~1.93 to ~1.87 Ga post-Waterberg dolerites. South African Journal of Geology, 107, 233-254.

Hanson, R. E., Harmer, R. E., Blenkinsop, T. G., Bullen, D. S., Dalziel, I. W. D., Gose, W. A., Hall, R. P., Kampunzu, A. B., Key, R. M., Muk wakwami, J., Munyanyiwa, H., Pancake, J. A., Seidel, E. K. & Ward, S. E. 2006. Mesoprotero zoic intraplate magmatism in the Kalahari Cra ton: A review. Journal of African Earth Sci ences, 46, 141-167.

Heaman, L. M. & LeCheminant, A. N. 1993. Paragene sis and U-Pb systematics of baddeleyite (Zr02). Chemical Geology, 110, 95-126.

Irvine, T.N. & Baragar, W.R.A. 1971. A guide to chemical classification of the common volcanic rocks. Canadian Journal of Earth Sciences, 8, 523-548.

Jensen, L.S. 1976. A new cation plot for classifying subalkalic volcanic rocks. Ministry of Natural resources. 22 pp.

Jourdan, F., Féraud, G., Bertrand, H., Kampunzu, A. B., Tshoso, G., Le Gall, B., Tiercelin, J. J. & Capiez, P. 2004. The Karoo triple junction ques tioned: evidence from Jurassic and Proterozoic 40Ar/39Ar ages and geochemistry of the giant Okavango dyke swarm (Botswana)□. Earth and Planetary Science Letters, 222, 989-1006.

Jourdan, F., Féraud, G., Bertrand, H., Watkeys, M. K., Kampunzu, A. B. & Le Gall, B. 2006. Base ment control on dyke distribution in Large Ig neous Provinces: Case study of the Karoo triple junction. Earth and Planetary Science Letters, 241, 307-322.

Klausen, M. B., Söderlund, U., Olsson, J. R., Ernst, R. E., Armoogam, M., Mkhize, S. W. & Petzer, G. 2010. Petrological discrimination among Pre cambrian dyke swarms: Eastern Kaapvaal cra ton (South Africa). Precambrian Research, 183, 501-522.

LeBas, M.J., LeMaitre, R.W., Streckeisen, A. & Zan ettin, B. 1986. A chemical classification of volcanic rocks based on the total alkali silica diagram. Journal of Petrology, 27, 745-750.

Li, Z. X., Bogdanova, S. V., Collins, A. S., Davidson, A., De Waele, B., Ernst, R. E., Fitzsimons, I. C. W., Fuck, R. A., Gladkochub, D. P., Jacobs, J., Karlstrom, K. E., Lu, S., Natapov, L. M., Pease, V., Pisarevsky, S. A., Thrane, K. & Vernik ovsky, V. 2008. Assembly, configuration, and break-up history of Rodinia: A synthesis. Pre cambrian Research, 160, 179-210.

Linström, D.R. 1987. 1:250 000 Geological map of South Africa. 2830 Dundee. Geological Survey of South Africa

Lubnina, N., Ernst, R., Klausen, M. & Söderlund, U. 2010. Paleomagnetic study of NeoArchean–Paleoproterozoic dykes in the Kaapvaal Craton. Precambrian Research, 183, 523-552.

Ludwig, K.R., 2003. Isoplot 3.00; A geochronological toolkit for Microsoft Excel. Berkely Geochro nological Center Publication No. 4.

Marsh, J. S. 2006. The Dominion Group. In: Johnson, M. R., Anhaeusser, C. R. & Thomas, R. J. (eds.) The Geology of South Africa. pp.149-154: The Geological Society of South Africa, Council for Geoscience.

McCarthy, T. S. 2006. The Witwatersrand Supergroup. In: Johnson, M. R., Anhaeusser, C. R. & Thomas, R. J. (eds.) The Geology of South Africa. pp. 155-186: The Geological Society of South Africa, Council for Geoscience.

McCourt, S., Armstrong, R. A., Grantham, G. H. & Thomas, R. J. 2006. Geology and evolution of the Natal belt, South Africa. Journal of African Earth Sciences, 46, 71-92.

McDonough, W.F. & Sun, S. S. 1995. The composition of the earth. Chemical Geology, 120, 223-253.

Mukasa, S. B., Wilson, A. H. & Young, K. R. 2013. Geochronological constraints on the magmatic and tectonic development of the Pongola Supergroup (Central Region), South Africa. Precambrian Research, 224, 268-286.

Nance, R. D., Murphy, J. B. & Santosh, M. 2014. The supercontinent cycle: A retrospective essay. Gondwana Research, 25, 4-29.

Olsson, J. R. 2012. U-Pb baddeleyite geochronology of Precambrian mafic dyke swarms and complexes in southern Africa - regional scale extensional events and the ogigin of Bushveld Complex, Lund, Lund University, 125

Olsson, J. R., Söderlund, U., Hamilton, M. A., Klausen, M. B. & Helffrich, G. R. 2011. A late Archaean radiating dyke swarm as possible clue to the origin of the Bushveld Complex. Nature Geoscience, 4, 5.

Olsson, J. R., Söderlund, U., Klausen, M. B. & Ernst, R. E. 2010. U–Pb baddeleyite ages linking major Archean dyke swarms to volcanic-rift forming events in the Kaapvaal craton (South Africa), and a precise age for the Bushveld Complex. Precambrian Research, 183, 490-500.

Stanistreet, I. G. & McCarthy, T. S. 1991. Changing tectono-sedimentary scenarios relevant to the development of the Late Archaean Witwatersrand Basin. Journal of African Earth Sciences (and the Middle East), 13, 65-81.

Sun, S.S. & McDonough, W.F. 1989. Chemical and isotopic systematics of oceanic basalts: implications for mantle composition and processes. In: Saunders, A.D. & Norry, M.J. (eds) Magmatism in the Ocean Basins, Geological Society Special Publications No 42. Pp. 313-345.

Svensen, H., Corfu, F., Polteau, S., Hammer, Ø. & Planke, S. 2012. Rapid magma emplacement in the Karoo Large Igneous Province. Earth and Planetary Science Letters, 325-326, 1-9.

Söderlund, U., Ibanez-Mejia, M., El Bahat, A., Ernst, R. E., Ikenne, M., Soulaimani, A., Youbi, N., Cousens, B., El Janati, M. h. & Hafid, A. 2013. Reply to Comment on "U–Pb baddeleyite ages and geochemistry of dolerite dykes in the Bas-Drâa inlier of the Anti-Atlas of Morocco: Newly identified 1380Ma event in the West African Craton" by André Michard and Dominique Gasquet. Lithos, 174, 101-108

Söderlund, U & Johansson, L. 2002. A simple way to extract baddeleyite (ZrO2). Geochemistry Geophysics Geosystems, 3,7.

Uken, R. & Watkeys, M. K. 1997. An interpretation of mafic dyke swarms and their relationship with major mafic magmatic events on the Kaapvaal Craton and Limpopo Belt. South African Journal of Geology, 100, 341-348.

Zhang, S., Li, Z.-X., Evans, D. A. D., Wu, H., Li, H. & Dong, J. 2012. Pre-Rodinia supercontinent Nuna shaping up: A global synthesis with new paleomagnetic results from North China. Earth and Planetary Science Letters, 353-354, 145-155.

Tidigare skrifter i serien ”Examensarbeten i Geologi vid Lunds universitet”:

356. Larsson, Emilie, 2013: Identifying the Cretaceous–Paleogene boundary in North Dakota, USA, using portable XRF. (15 hp)
357. Anagnostakis, Stavros, 2013: Upper Cretaceous coprolites from the Münster Basin (northwestern Germany) – a glimpse into the diet of extinct animals. (45 hp)
358. Olsson, Andreas, 2013: Monazite in metasediments from Stensjöstrand: A pilot study. (15 hp)
359. Westman, Malin, 2013: Betydelsen av raka borrhål för större geoenergisystem. (15 hp)
360. Åkesson, Christine, 2013: Pollen analytical and landscape reconstruction study at Lake Storsjön, southern Sweden, over the last 2000 years. (45 hp)
361. Andolfsson, Thomas, 2013: Analyses of thermal conductivity from mineral composition and analyses by use of Thermal Conductivity Scanner: A study of thermal properties in Scanian rock types. (45 hp)
362. Engström, Simon, 2013: Vad kan inneslutningar i zirkon berätta om Varbergscharnockiten, SV Sverige. (15 hp)
363. Jönsson, Ellen, 2013: Bevarat maginnehåll hos mosasaurier. (15 hp)
364. Cederberg, Julia, 2013: U-Pb baddeleyite dating of the Pará de Minas dyke swarm in the São Francisco craton (Brazil) - three generations in a single swarm. (45 hp)
365. Björk, Andreas, 2013: Mineralogisk och malmpetrografisk studie av disseminerade sulfider i rika och fattiga prover från Kleva. (15 hp)
366. Karlsson, Michelle, 2013: En MIFO fas 1 -inventering av förorenade områden: Kvarnar med kvicksilverbetning Jönköpings län. (15 hp)
367. Michalchuk, Stephen P., 2013: The Säm fold structure: characterization of folding and metamorphism in a part of the eclogite-granulite region, Sveconorwegian orogen. (45 hp)
368. Praszkier, Aron, 2013: First evidence of Late Cretaceous decapod crustaceans from Åsen, southern Sweden. (15 hp)
369. Alexson, Johanna, 2013: Artificial groundwater recharge – is it possible in Mozambique? (15 hp)
370. Ehlorsson, Ludvig, 2013: Hydrogeologisk kartering av grundvattenmagasinet Åsumsfältet, Sjöbo. (15 hp)
371. Santsalo, Liina, 2013: The Jurassic extinction events and its relation to CO_2 levels in the atmosphere: a case study on Early Jurassic fossil leaves. (15 hp)
372. Svantesson, Fredrik, 2013: Alunskiffern i Östergötland – utbredning, mäktigheter, stratigrafi och egenskaper. (15 hp)
373. Iqbal, Faisal Javed, 2013: Paleoecology and sedimentology of the Upper Cretaceous (Campanian), marine strata at Åsen, Kristianstad Basin, Southern Sweden, Scania. (45 hp)
374. Kristinsdóttir, Bára Dröfn, 2013: U-Pb, O and Lu-Hf isotope ratios of detrital zircon from Ghana, West-African Craton – Formation of juvenile, Palaeoproterozoic crust. (45 hp)
375. Grenholm, Mikael, 2014: The Birimian event in the Baoulé Mossi domain (West African Craton) — regional and global context. (45 hp)
376. Hafnadóttir, Marín Ósk, 2014: Understanding igneous processes through zircon trace element systematics: prospects and pitfalls. (45 hp)
377. Jönsson, Cecilia A. M., 2014: Geophysical ground surveys of the Matchless Amphibolite Belt in Namibia. (45 hp)
378. Åkesson, Sofia, 2014: Skjutbanors påverkan på mark och miljö. (15 hp)
379. Härling, Jesper, 2014: Food partitioning and dietary habits of mosasaurs (Reptilia, Mosasauridae) from the Campanian (Upper Cretaceous) of the Kristianstad Basin, southern Sweden. (45 hp)
380. Kristensson, Johan, 2014: Ordovicium i Fågelsångskärnan-2, Skåne – stratigrafi och faciesvariationer. (15 hp)
381. Höglund, Ida, 2014: Hiatus - Sveriges första sällskapsspel i sedimentologi. (15 hp)
382. Malmer, Edit, 2014: Vulkanism - en fara för vår hälsa? (15 hp)
383. Stamsnijder, Joaen, 2014: Bestämning av kvartshalt i sandprov - medtodutveckling med OSL-, SEM– och EDS-analys. (15 hp)
384. Helmfrid, Annelie, 2014: Konceptuell modell över spridningsvägar för glasbruksföroreningar i Rejmyre samhälle. (15 hp)
385. Adolfsson, Max, 2014: Visualizing the volcanic history of the Kaapvaal Craton

using ArcGIS. (15 hp)

386. Hajny, Casandra, 2014: Ett mystiskt ryggradsdjursfossil från Åsen och dess koppling till den skånska, krittida ryggradsdjursfaunan. (15 hp)
387. Ekström, Elin, 2014: – Geologins betydelse för geotekniker i Skåne. (15 hp)
388. Thuresson, Emma, 2014: Systematisk sammanställning av större geoenergianläggningar i Sverige. (15 hp)
389. Redmo, Malin, 2014: Paleontologiska och impaktrelaterade studier av ett anomalt lerlager i Schweiz. (15 hp)
390. Artursson, Christopher, 2014: Comparison of radionuclide-based solar reconstructions and sunspot observations the last 2000 years. (15 hp)
391. Svahn, Fredrika, 2014: Traces of impact in crystalline rock – A summary of processes and products of shock metamorphism in crystalline rock with focus on planar deformation features in feldspar. (15 hp)
392. Järvin, Sara, 2014: Studie av faktorer som påverkar skredutbredningen vid Norsälven, Värmland. (15 hp)
393. Åberg, Gisela, 2014: Stratigrafin i Hanöbukten under senaste glaciationen: en studie av borrkärnor från IODP's expedition nr 347. (15 hp)
394. Westlund, Kristian, 2014: Geomorphological evidence for an ongoing transgression on northwestern Svalbard. (15 hp)
395. Rooth, Richard, 2014: Uppföljning av utlastningsgrad vid Dannemora gruva; april 2012 - april 2014. (15 hp)
396. Persson, Daniel, 2014: Miljögeologisk undersökning av deponin vid Getabjär, Sölvesborg. (15 hp)
397. Jennerheim, Jessica, 2014: Undersökning av långsiktiga effekter på mark och grundvatten vid infiltration av lakvatten – fältundersökning och utvärdering av förhållanden vid Kejsarkullens avfallsanläggning, Hultsfred. (15 hp)
398. Särman, Kim, 2014: Utvärdering av befintliga vattenskyddsområden i Sverige. (15 hp)
399. Tuvesson, Henrik, 2014: Från hav till land – en beskrivning av geologin i Skrylle. (15 hp)
400. Nilsson Brunlid, Anette, 2014: Paleoekologisk och kemisk-fysikalisk undersökning av ett avvikande sedimentlager i Barsebäcks mosse, sydvästra Skåne, bil dat för ca 13 000 år sedan. (15 hp)
401. Falkenhaug, Jorunn, 2014: Vattnets kretslopp i området vid Lilla Klåveröd: ett kunskapsprojekt med vatten i fokus. (15 hp)
402. Heingård, Miriam, 2014: Long bone and vertebral microanatomy and osteohistology of 'Platecarpus' ptychodon (Reptilia, Mosasauridae) – implications for marine adaptations. (15 hp)
403. Kall, Christoffer, 2014: Microscopic echinoderm remains from the Darriwilian (Middle Ordovician) of Västergötland, Sweden – faunal composition and applicability as environmental proxies. (15 hp)
404. Preis Bergdahl, Daniel, 2014: Geoenergi för växthusjordbruk – Möjlig anläggning av värme och kyla i Västskåne. (15 hp)
405. Jakobsson, Mikael, 2014: Geophysical characterization and petrographic analysis of cap and reservoir rocks within the Lund Sandstone in Kyrkheddinge. (15 hp)
406. Björnfors, Oliver, 2014: A comparasion of size fractions in faunal assemblages of deep-water benthic foraminifera—A case study from the coast of SW-Africa.. (15 hp)
407. Rådman, Johan, 2014: U-Pb baddeleyite geochronology and geochemistry of the White Mfolozi Dyke Swarm: unravelling the complexities of 2.70-2.66 Ga dyke swarms on the eastern Kaapvaal Craton, South Africa. (45 hp)

LUNDS UNIVERSITET

Geologiska institutionen
Lunds universitet
Sölvegatan 12, 223 62 Lund